AD615307

(1)

NRL Memorandum Report 1483

LASER MATERIALS RESEARCH

REPORT OF PROGRESS 1 JULY 1963 - 15 DECEMBER 1963

45-p

COPY	1	OF	1
HARD COPY		$. 2.00	
MICROFICHE		$. 0.50	

DECEMBER 1963

DEPARTMENT OF THE NAVY
OFFICE OF NAVAL RESEARCH

U. S. NAVAL RESEARCH LABORATORY
Washington, D.C.

LASER MATERIALS RESEARCH

REPORT OF PROGRESS 1 JULY 1963 - 15 DEC 1963

Introduction

NRL Memorandum Report 1442 summarized the studies carried out jointly by the Solid State, Optics, and Radiation Divisions of the U. S. Naval Research Laboratory during the period 1 Jan 1963 to 30 June 1963 on a program of laser materials research partially supported by ARPA Order No. 306, monitored by the Physics Branch of the Office of Naval Research. The present report summarizes the progress made from 1 July 1963 to 15 December 1963. During this period work was carried out on the following:

1. Evaluation of the optical quality of synthetic rubies.
2. Investigation of the ^2E levels of ruby.
3. The optical absorption spectrum of ruby.
4. Investigation of excited-state absorption in gadolinium-activated glass.
5. Spectroscopy of ytterbium-activated laser glass.
6. The synthesis of laser glasses, particularly of gadolinium and europium activated glasses.
7. Investigation of the light emission produced by double-pulsing of flash lamps.
8. Continued studies on optical pumping using exploding wire light sources.
9. Fundamental investigations of pumping light sources.
10. Observations of effects due to high intensity laser beams.

Progress in these areas is described below.

1. Evaluation of Optical Quality of Synthetic Rubies. (Radiometry Branch, Optics Division.)

Ruby used in the ARPA laser program has been far inferior to glass in optical quality, and requires substantial improvement for theoretical laser performance to be achieved. Efforts are being made by the suppliers of ruby to synthesize material of greater uniformity. NRL is helping to monitor this program by conducting optical tests on samples submitted through ONR. The tests conducted up to this time have been limited by the quality of the material and the physical condition of the samples. Interferometric techniques could not be applied to the rough samples submitted and they would have been unduly sensitive to the observed gross variations in refractive index. These techniques are being applied to the samples after optical finishing and will become increasingly useful as quality improves.

The samples received to date have been rough cuts from boules grown by the Linde Co. and Thermal Syndicate and crystals flux grown by Airtron (Fig. 1). Preliminary measurements were made on the crystals as received by immersing them in diiodemethane for index matching.

The optic axis pattern was examined with convergent light and crossed polarizers (Fig. 2) and the direction of the optic axis referenced. The elements of the dark cross in the optic axis pattern, (Fig. 3A) are referred to as the isogyres. This particular figure is an example of how the optic axis pattern of an ideal uniaxial crystal should look. The uniformity of the isogyres is indicative of the uniformity of direction of the optic axis. The position of the cross in the field indicates the deviation of the optic axis from the line of sight. The dark circles are interference fringes, and represent lines of equal phase difference between the ordinary and extra-ordinary waves. They are indicative of axis uniformity but, unlike the isogyres, they are also affected by variations in refractive index and by surface conditions. The optic axis patterns for the boules (Fig. 4) were in general poor by comparison with those for the flux grown ruby. It might be noted that the equilateral hyperbola type of isogyre pattern, Fig. 4, Linde No. 1830-16, for example, is characteristic of a biaxial crystal.

Small angle scattering along the optic axis was studied by projecting the diffraction pattern of a 1/4 inch aperture illuminated by a distant point source, (Figs. 5, 6, 7, 3B). An exposure range of 6000 times was used in these figures to show intensity as a function of angle. The shortest exposure with no sample shows just the central maximum, 10^{-4} radians in diameter, and indicates the angular scale. The Thermal Syndicate No. 636 sample was subsequently cut into a cube and finished for the pictures in Fig. 7. In this instance the 6328A line from a helium-neon gas laser was used to illuminate the aperture.

The Airtron flux-grown ruby shows the greatest uniformity of crystal structure. The moderate amount of small angle scatter observed, is believed to be due to surface variations. Index matching was not perfect and refraction at the multiplanar surfaces would account for this scatter. Thermal Syndicate No. 636 had a very poor optic axis figure and yet showed the least small-angle scatter of any sample. One can only conclude that the scattering observed was not primarily associated with non-uniformity of optic axis direction.

Shadowgraphs were made with essentially parallel light from a distant point source (Fig. 8). These show gross variations in the index of refraction and suggest the cause of the observed scatter. Here no optics are used, but the rays from a point source are bent slightly by index variations in the ruby to produce the resultant patterns (Figs. 9, 10A, 10B, 10C).

A similar physical arrangement (Fig. 11) is used for the examination with crossed polaroids (Figs. 12, 4A, 10D). The light passing through the crystal is essentially parallel so the crystal should appear of uniform optical density except as a result of strain and axis variation. Visual inspection suggests that variation in chromium content is a major factor in index variation. Examination of the ruby samples by phase microscopy showed the presence of some inclusions and microscopic defects.

Optical finishing of the samples is being completed and additional tests will be made when the finished samples are received.

2. <u>Investigation of the ^2E Levels of Ruby</u>. (Radiometry Branch, Optics Division).

Resonance scattering by the ^2E levels and thermal relaxation between the two ^2E levels are being investigated. The purpose of this investigation is twofold. For the optical quality evaluation it was necessary to know the contribution of resonance scatter to wide angle scatter for wavelengths in the vicinity of the R_1 line. A second purpose of this investigation is to look into the possibility of pumping the lower ^2E level with the output of an R_2 line laser. Such a pumping scheme would essentially eliminate the pump cycle heating problem and the problem of maintaining the optical integrity of a ruby laser during the pumping period (Fig. 13).

Two types of experiments were performed. For one, ruby at room temperature was irradiated by ruby laser light (Fig. 14), and high resolution spectra were made of the R_1 and R_2 lines from the irradiated ruby. By cooling the ruby laser to 100°K it was possible to shorten the wavelength of the exciting radiation to a point midway between the room temperature R_1 and R_2 lines. Excitation of the R_1 and R_2 lines decreased equally as the wavelength was shortened and no change was noted in the relative appearance of the R_1 and R_2 lines. The line due to scattered excitation radiation remained sharp in all cases .

In the second type of experiment the ruby was irradiated by a Q-switched laser and the spectrograph was used as a monochromator with an output slit and photomultiplier (Fig. 15). A vacuum photo-diode monitored the pulses from the Q-switched laser and the two outputs were displayed on a dual beam oscilloscope. The monochromator was tuned to various wavelengths in the vicinity of the R_1 and R_2 lines and photo-oscillograms were made showing the time relation between the excited radiation and the exciting pulses (Fig. 16). It was found that at room temperature the thermal filling of the upper ^2E level from the lower takes place in less than 10^{-7} seconds. This experiment will be repeated at various low temperatures and this relaxation time determined as a function of temperature. If R_2 line pumping is to be successful, the lower to upper relaxation time must be much longer than the inverse decay relaxation time. If the results of the low temperature measurements are encouraging, and R_2 line laser at the appropriate temperature will be used to study the upper-to-lower relaxation time.

3. Optical Absorption in Ruby. (Dielectrics Branch, Solid State Division).

The observation of enhanced U. V. optical absorption from the ^2E radiating states to higher lying states was reported in NRL Memorandum Report 1442. It was pointed out that the importance of this type of depopulation of the ^2E states by the ultraviolet spectral components of the flashlamp will depend upon whether or not electrons excited to the higher lying states ($\bar{\nu} \gtrsim 35000 cm^{-1}$) return to the ^2E levels, and on the relative magnitude of the time constants for the several possible electronic transitions. Extension of the enhanced absorption measurements to longer wavelengths was interrupted in order to perform the optical evaluation described under Item 1 above. However, optical absorption studies of ruby were continued, in an attempt to understand the origin of the high-lying energy states involved in this absorptive depopulation of the radiating states.

A number of crystals of ruby of different concentrations and orientations were purchased from commercial suppliers. These crystals were grown by the flame-fusion method; an unpolished zero degree ruby plate grown by the flux technique by the Airtron Company was also used in this study. Parallel-faced optical absorption pieces of different thicknesses were prepared from each ruby sample. The room-temperature optical absorption spectra of the zero-degree oriented samples (optic axis perpendicular to the slab face) were obtained using the unpolarized radiation in a Cary Model 14M Recording Spectrophotometer.

The optical absorption spectrum (uncorrected for reflection losses) of a Meller 0.04% ruby sample is shown in Figure 17. The familiar absorption spectrum of ruby in the visible and near ultraviolet was observed. The absorption spectra observed for the other samples was qualitatively similar to the one shown except that the band centered around 3150A was detected only in the 0.04% Meller crystals. Since it was found that the optical absorption coefficient at 5600A for the Meller 0.04% crystals and the Linde 0.04% crystal differed by about 60%, a correlation plot was made in Figure 18, using the optical absorption coefficient at 5600A as the abscissa and optical absorption coefficients of other band maxima as ordinates. It is assumed that the abscissa is proportional to Cr^{+3} concentration.

Curve A shows a plot of the 4100A absorption coefficient as the ordinate. It is seen that the points fall accurately on a straight line of unit slope. This shows that the 4100A band is correlated with the 5600A band, and, by assumption, is linearly related to Cr^{+3} concentration in the crystal. Curve (B) is a correlation plot of the 2580A absorption coefficient and it is seen to follow a 45° line at the lower concentrations and approach a straight line of slope 2 at higher concentrations. A slope of 2 would indicate a dependence upon the square of the concentration. Linz and Newnham[1] have shown a square law concentration dependence for a group of

---

[1] A. Linz Jr., and R. E. Newnham, Phys. Rev. 123, 500 (1961)

---

absorption bands around 3400A, but in a higher concentration range than studied here. Certain emission lines in higher concentration ruby have been ascribed to coupled chromium ion pairs by Schawlow et al.[2]

---

[2] A. T. Schawlow, D. L. Wood and A. M. Clogston, Phys. Rev. Letters 3, 271 (1959).

The absorption at 2100A is shown plotted against relative concentration in curve C of Figure 2. It seems clear that neither curve (B) nor curve (C) correlate well with a linear concentration Cr^{+3} dependence. It would seem that these bands are due to chromium in some state of pairing or other aggregation.

A Meller 0.04% zero-degree ruby etalon was exposed to ~100 Mr of Cs^{137} gamma irradiation (0.68 Mev) at a rate of 0.25 Mr per hour. The etalon was tightly wrapped with aluminum foil to prevent deterioration of the reflecting surfaces by ozone or other radiation-produced active chemicals. It was found that the irradiated ruby had a distinct orange appearance, and its spontaneous emission was reduced. The etalon was pulse-excited with a Xenon flashlamp, and the threshold for spiking was found to be about twice that of the unirradiated etalon. After twelve excitations using progressively decreasing lamp voltage, the original unirradiated threshold for spiking was observed, and the etalon no longer appeared orange in color. This suggests that the reflecting films were not significantly damaged in the gamma irradiation and that the induced optical absorption is optically bleachable by broadband radiation.

All of the zero-degree ruby absorption samples were irradiated with the same Cs^{137} source, and were exposed to 125 Mr of this radiation. Optical absorption measurements were made before and after this irradiation and the induced optical absorption coefficients for each sample are shown in the semilog plots of Figure 19. A broad maximum is found in each sample centered around 4700A with induced absorption coefficient of about 4 cm^{-1} for the higher concentration samples. Since this absorption is larger than the Cr^{+3} pump bands in the visible, it is believed that the induced band competes with the Cr^{+3} bands for the flashlamp radiation in this spectral region and thereby causes the observed increase in the spiking threshold for the irradiated ruby etalon. In every case, the induced absorption coefficient at the ruby laser wavelength is considerably less than 0.1 cm^{-1}. By far the largest absorption is induced in the ultraviolet spectral region (below 3000A). It should be noted that unactivated corundum showed no measurable induced optical absorption for the same radiation exposure.

In Fig. 20, the concentration-dependence of the induced absorption shows that a maximum value of induced absorption at different wavelengths is achieved around the Linde 0.04% concentration for the exposure given the samples. Absorption growth-curve studies might be helpful in ascertaining whether the induced absorption really achieves a maximum at different concentrations for the different wavelengths.

Preliminary measurements of the optical absorption spectra of unirradiated Meller 0.005% ruby have been made in the vacuum ultraviolet spectral region. This low resolution spectrum is given in Fig. 21 and shows a broad band centered around 1800A. The absorption coefficient at this band maximum is about 50 cm^{-1}, which is about two orders of magnitude greater than the visible absorption. This suggests the optical absorption cross section is in the order of 10^{-16} cm^2, which implies a highly allowed transition (oscillator strength in the order of unity). This in turn strongly suggests that the optical transition is of the charge transfer type. Optical absorption measurements will be continued in this spectral region when suitable samples are prepared.

4. Studies of Excited-State Absorption in Gadolinium-Activated Glass. (Dielectrics Branch, Solid State Division)

Stimulated near-ultraviolet emission was found to take place in a gadolinium activated glass developed at this Laboratory, but the observed output was of a low grade type in which off-axis modes dominated.[1,2]

[1] H. W. Gandy and R. J. Ginther, J. Appl. Phys. Ltrs. 1:25 (1963)

[2] H. W. Gandy and R. J. Ginther, "Stimulated Emission of Ultraviolet Radiation from Gadolinium-Activated Glass" Third International Congress on Quantum Electronics, Paris, France, February 11-15, 1963.

In a continuing study of this material, it seemed worthwhile to assay the magnitude of the enhanced absorption in gadolinium-activated glasses (Process C in Fig. 22) and its possible effect upon stimulated emission. This investigation parallels work reported in NRL Memorandum Report 1442 on enhanced absorption in ruby.

The optical absorption (and excitation) spectra of gadolinium in the two glass compositions to be reported here consist of a series of low-oscillator-strength narrow bands in the region between 3200A and 2400A, with strong luminescence taking place around 3130A. The emission lifetime is about 3.8 msec in the $LiMgAlSiO_3$ glass. The gadolinium absorption spectra are rather similar. In the former glass, the quantum efficiency for luminescence is near unity. It is noteworthy that five gadolinium absorption bands nearly coincide with mercury emission lines.

It is impossible to detect higher-lying localized gadolinium levels in these glasses by direct optical absorption techniques because strong absorption in the unactivated glasses starts around 2100A. Hence there is no way of evaluating the enhanced absorption effect because of lack of knowledge of the spectral position and intensities of possible higher excited states; one must then resort to methods of excited-state absorption spectroscopy.

The schematic arrangement of the experimental apparatus used in this study is shown in Fig. 23. A polished block of the sample glass is mounted in front of the spectrograph on one end of a hollow metal tube which serves not only as a support but also as an aperture for the system. A mercury flashtube is used to build up the population in the $^6P_{7/2}$ radiating state in the sample. A broad-band xenon flashlamp is focussed on the glass block and is used (with the spectrograph) to ascertain changes in the optical transmission of the glass upon irradiation by the mercury lamp. If absorption were to take place between the radiating state and the known higher-lying states in this ion, it should occur in the infrared, with absorption to the highest lying state of this ^6I multiplet possibly occurring around 1.26μ and absorption to the other states lying at longer wavelengths; hence these transitions can not be observed photographically. If, however, absorption takes place from the radiating state to the spectral vicinity of the absorption edge of the glass itself, it should commence around 6700A and could persist to shorter wavelengths; this could be photographically detected. Since wavelengths down to 2200A can be detected photographically this would correspond to levels lying 79,000 cm^{-1} above the ground state or about 1250A in direct absorption.

Single-flash and multiple-flash sequence exposures were made with both glass samples. The time sequence of flashlamp radiation for each spectral line was detected with a photodiode (RCA-935 with Corning 9862 filter) and recorded oscillographically. This record can insure a correct photographic intensity evaluation from one flash sequence to the next. A typical flash sequence is shown in Fig. 24. First the xenon and mercury flashtubes were fired individually at a predetermined level and their spectra photographed individually. The mercury flash spectra give an indication of the strong gadolinium luminescence and the strength of the light scattered into the spectrograph by the sample. Next, the xenon lamp was fired at the beginning of the long mercury pulse, and the spectra photographed. Then the mercury lamp was flashed and, after a prolonged delay the interrogating xenon lamp was flashed, and the spectrum sequence photographed. The densitometer trace of the latter sequence is then subtracted from the previous one over the aforementioned wavelength region. Presumably, the decrease in the transmission of the mercury-pumped sample is then due to absorption from the radiating state.

The mercury tube was always fired with a 570 μH inductance and at 400 v or 500 v stored on a capacitor bank having capacities as high as 1120 μf; its flash duration was in the neighborhood of 1 to 2 msec. The xenon flashtube was fired with no inductance and with 1.2 kv stored on 48-μf capacity its flash duration was around 50-80 μ sec. It is estimated that somewhere in the order of 1% of gadolinium ions were in the radiating state under most of the conditions of experimentation.

In the region below about 6000A in the delayed-interrogation pulse spectra, it was found that the $LiMgAlSiO_3$ glass absorption was increased by approximately 3% to 5%, whereas the $LiCaAlSiO_3$ glass absorption was increased by approximately 7%. Although these differences are about the same as the experimental errors expected in this measurement, it was noted that the rich ultraviolet content of the mercury flashlamp caused radiation damage (increased-background optical absorption) in the ultraviolet region, which extended with decreasing intensity throughout the visible region. This effect was greater with the latter glass than with the former. This increased background absorption (as measured from the ground state, not the radiating state) could account for a good part of the absorption increase observed.

From these results it seems that, at the excitation level at which these experiments were carried out, any enhanced absorption from the radiating state to higher-lying states was several percent or less. Under comparable excitation conditions, the effect in ruby could be an order of magnitude larger.

From this negative result it should not be inferred that this excited-state absorption effect is negligible in these materials at all levels of excitation. These experiments will be repeated when a more intense ultraviolet excitation source is developed for this work.

5. Spectroscopy Studies of Ytterbium-Activated $LiMgAlSiO_3$ Glass. (Dielectrics Branch, Solid State Division)

Study of the spectroscopy of ytterbium in $LiMgAlSiO_3$ glass has been continued in the attempt to understand the factors which control the various optical parameters of this activator, and to determine the influence of the host matrix upon the stimulated emission.

As discussed in NRL Memorandum Report 1442, the luminescence spectrum of this glass contains two bands whose maxima are located at 0.976μ (~60A band width) and 1.02 μ (600A band width at room temperature). Stimulated emission is observed in the latter at 80°K. The former band has tentatively been associated as an unresolved doublet from the M=5/2 component of the $^2F_{7/2}$ ground state to the M=3/2 and 5/2 levels of the excited $^2F_{5/2}$ multiplet of $Yb^{+3}(4f^{13})$ which has been observed in several crystal systems.[1,2,3,4,5]

[1]G. H. Dieke and A. M. Crosswhite, J. Opt. Soc. Am. 46, 885(1956).

[2]P. P. Feofilov, Optics and Spectroscopy 5, 216 (1958).

[3]R. Pappalardo and D. L. Wood, J. Chem. Phys. 33, 1734 (1960).

[4]W. Low, Phys. Rev. 118, 1608(1960).

[5]W. Low, J. Chem. Phys. 37, 30(1962).

A schematic representation of the energy level diagram for Yb^{+3} is depicted in Figure 25. At present only a qualitative insight is sought within this framework because even at helium temperatures, the observed Yb^{+3} absorption and emission bands are rather broad in this glass host as compared to crystalline matrices. Together with the possibility of several different crystalline field positions of the ion, this precludes any detailed attempt to fit theory at the present time.

Nevertheless, our inability to understand the 1.02μ emission band led to a careful remeasurement of the luminescence from glass as a function of ytterbium concentration. The use of the 0.976μ emission band as an internal concentration index of Yb^{+3} led to considerable difficulty, for both optically and x-ray excited luminescence, because of it's large self-absorption. The x-ray excited luminescence spectrum of the glass in powdered form was given in NRL Memorandum Report 1442. This type of measurement was extended to several concentrations at room temperature with good geometry control and lower x-ray tube voltage. The peak of the 0.976 and 1.02μ emission bands thus obtained are plotted as a function of the log of the ytterbium concentration in Figure 26. The room temperature half widths of these bands do not vary significantly with concentration. Concentration quenching of both emission bands is apparent; and this quenching can be associated with the decrease of the decay time of the 1.02μ band shown in Figure 27. The decay time of 0.976μ band was measured using a monochromator in tandem with an interference filter and was found to be, within experimental error, the same as the 1.02μ band. Furthermore these two decay times decrease with temperature in about the same way, i.e. from 1400μ seconds at room temperature to 1250μ seconds at liquid helium temperature.

Referring again to Figure 26, curve 3 represents the ratio of the peak of the 1.02μ band to that of the 0.976μ band as a function of ytterbium concentration. Curve 4 represents the same ratio but with a self-absorption correction made for both bands using the x-ray penetration depth. This correction amounted to at most about 15%. These data were repeated using ultraviolet excitation, and similar results were obtained. Somewhat larger self absorption corrections were necessary in this case because of the greater penetration of the ultraviolet radiation. Although x-ray irradiation does induce optical absorption in the ultraviolet and visible spectral regions, no such absorption could be detected for comparable doses in a control sample for wavelengths longer than 0.75μ. If the 1.02μ band were directly proportional to the 0.976μ band, Curve 5 would result, leading to the conclusion that the 1.02μ as well as the 0.976μ emission is directly proportional to Yb^{+3}. The experimental Curve (4) shows that this is not the case; at a Yb^{+3} concentration of 0.02, Curve 4 exceeds Curve 5 by almost a factor of 2, which implies about 100% more 1.02μ radiation is being observed than would be expected if the origin of this band were due only to individually dispersed Yb^{+3} ions in the glass.

It should be noted that this type of concentration dependence is not observed in the room-temperature absorption spectra, as may be seen by examining the correlation plots shown in Fig. 28, in which the absorption coefficients for wavelengths of 0.94, 0.976 and 1.0μ are plotted against concentration. A straight line of unit slope fits these data rather well for both CO-melted and air-melted glass samples, indicating the same concentration dependence and direct proportionality to Yb^{+3}. The half width of the 0.976μ band varies by 5% or less over the concentration range shown in Fig. 28.

As has been mentioned before, the absorption and emission at 0.976μ behave like a resonance transition, which probably takes place from the lowest lying components of the ground multiplet to the lower-lying levels of the excited multiplet. The broad absorption bands at 0.946 and 0.916μ probably take place at higher levels in the excited multiplet. Although these levels are 340 cm^{-1} and 680 cm^{-1}, respectively, above the lowest state, the absence of strong temperature-dependence in these bands suggests that they probably are not associated with phonon-assisted electronic transitions involving the resonance absorption at 0.976μ. The observation that the 1.02μ and 0.976μ emission bands both possess the same decay time, suggests that both bands originate from the same upper energy state(s). If this is the case, the 1.02μ band terminates on energy levels whose center of gravity is about 390 cm^{-1} above the ground multiplet. Since the 1.02μ band shows abnormally large concentration dependence, it is possible that these terminal levels result from some condition of aggregation, or near aggregation, of ytterbium ions in this glass.

A situation somewhat similar to this has been reported for higher concentration ruby.[6] Schawlow et al. postulate that exchange coupling

---

[6] A. L. Schawlow, D. L. Wood and A. M. Clogston, Phys. Rev. Letters, 3, 271 (1959).

---

between paired Cr^{+3} ions removes the spatial degeneracy in the ground state. Although the sitiuation in the glass appears similar, it may not be quite so simple.

The absorption spectrum of the ytterbium-activated glass was measured in the temperature range from about 10°K to about 800°K in an attempt to confirm the energy separation of the terminal and ground states in the laser transitions and to determine the optical cross-section of these transitions. These data are not yet fully reduced, but a preliminary rough estimate yields a cross-section for optical absorption (and hence for stimulated emission) in the order of 10^{-20} cm^2. The difference between the absorption spectra at 300°K and liquid nitrogen temperature shows a weak band in the vicinity of 1μ, suggesting optical absorption is taking from thermally populated states to higher lying states.

The d bands for this ion have not been unequivocally observed in this glass. But additional, structureless absorption, superimposed on the tail of the fundamental glass absorption and extending to the vicinity of 3500A, may be the side of a strong d band whose maxima lies to wavelengths shorter than the absorption edge of the host glass, i.e., 2100A. Excitation spectrum measurements for 1.02μ luminescence reinforce this hypothesis. It is not surprising that the position of this band does not agree with the 2500A d band reported by Feofilov[2] for $CaF_2:Yb^{3+}$, because the 5d states are unshielded by the completed $5S^2$

and $5P^6$ electronic configuration of the xenon case, and hence can be influenced significantly by the crystalline field environment of the host matrix. It may be noted, however, that a band which could be associated with Yb^{+2} was observed in the CO-melted glass at 3300A whereas Feofilov reported a Yb^{+2} band at 3600A in CaF_2. Initial measurements probing the 3600A region for excitation of the 1.02μ luminescence failed to show any evidence for transfer of energy absorbed in the divalent ion to the trivalent ion. A search in the ultraviolet spectral region indicated no short wavelength luminescence associated with the d band excitation of the 1.02μ band, i.e., no radiative transitions from the d bands to the $^2F_{5/2}$ multiplet.

The evidence reported here for ytterbium in $LiMgAlSiO_3$ glass suggests that the spontaneous emission decay time is more sensitive to host environment than optical absorption this is observed to a greater or lesser degree in many phosphor systems.

6. Synthesis of Laser Glasses. (Dielectrics Branch, Solid State Division).

The greatest proportion of the effort on glass synthesis in this period has been devoted to the improvement of gadolinium-activated glass. The failure of this glass to provide a spiking pattern of laser oscillations had been attributed to a combination of poor optical quality, inefficient excitation from conventional flash lamps, and competition for absorbed energy by europium impurity in the gadolinium oxide raw material. The program to provide more efficient excitation of this glass by the technique of double pulsing of flashlamps is described in another section of this report. The present section describes attempts to improve glass quality and to eliminate the harmful effects of europium impurity.

The earliest attempt to improve glass quality consisted of efforts to produce larger batches of the Gd-activated $LiMgAlSiO_3$ glass by mixing and melting small melts. This failed to produce improved optical quality because the high viscosity of the melt did not permit good mixing, and because the glass is not a particularly stable one, large pieces tending to devitrify upon annealing.

Modifications of the glass composition were then made in order to improve the above properties and it was found that altering the composition from

0.26 MgO		0.11 MgO
0.13 $LiO_{0.5}$		0.22 $LiO_{0.5}$
0.10 $AlO_{1.5}$	to	0.20 $AlO_{1.5}$
0.01 $GdO_{1.5}$		0.01 $GdO_{1.5}$
0.50 SiO_2		0.46 SiO_2

both lowered the viscosity and increased stability, and that larger pieces of the latter composition could in all probability be prepared. However in light of the results of some work on radiation damage to this glass, the $LiMgAlSiO_3$ system did not appear to be the most promising prospect.

A second type of glass tested early in this period is a Gd-activated $LiCaAlSiO_3$. This is not simply the calcium analog of the magnesium-containing glass used previously, but is of the composition:

$0.14\ CaO$
$0.15\ LiO_{.5}$
$0.40\ AlO_{1.5}$
$0.01\ GdO_{1.5}$
$0.30\ SiO_2$

This glass not only contains calcium instead of magnesium but is of higher alumina and lower silica content. It has a lower viscosity than the magnesium glass and appears to provide better glass quality. However the ultraviolet absorption of the calcium glass at about 2450A (the base glass absorption) is about twice that of the magnesium glass. Consequently an investigation was made in order to determine whether this increased absorption is due to impurities in the calcium carbonate or aluminum oxide raw materials, or whether it is a property of the glass composition itself. This investigation has demonstrated that impurities in the calcium carbonate were not responsible, and that if the aluminum oxide were suspect, no better source than the originally used material had been found. Meanwhile, radiation damage studies of this glass revealed that it, too, was probably not the best prospective host for gadolinium.

The technique of double pulsing flashlamps, described elsewhere in this report, gives promise of providing a more efficient excitation of gadolinium glasses, but an undesirable consequence of the use of this technique is that the glasses suffer radiation damage from the high intensity of ultraviolet light in the neighborhood of 2500A. The aluminosilicate glasses previously described exhibit this behavior to a considerable degree, and consequently a search for a more radiation-sensitive glass has been started. The most promising glass composition to date with regard to this property is a soda-lime glass containing no aluminum. The superiority of this glass can be seen from the following table in which the increased absorption produced by an exposure of 0.182 mega-rad Co^{60} dose is tabulated for three wavelengths.

Increased Absorption Produced by 0.182 mega-rad of Co^{60} at Indicated Wavelength

	2450A	2740A	3130A
LiMgAl Silicate	2.9 cm^{-1}	2.95 cm^{-1}	2.93 cm^{-1}
LiCaAl Silicate	2.52 cm^{-1}	2.58 cm^{-1}	2.29 cm^{-1}
NaCa Silicate	1.73 cm^{-1}	1.70 cm^{-1}	1.71 cm^{-1}

The improvement provided by the soda-lime glass is apparent, but the radiation damage effect is still rather large. It is not likely that this effect can be completely eliminated without adding "protective" ions such as cerium, which in all probability would be deleterious to the gadolinium luminescence.

The third deteriment to gadolinium laser glasses, the presence of europium impurity, as well as the reported success of europium chelates as lasers, has occasioned an investigation of the properties of europium-activated glasses. In order to obtain good ultraviolet transmission in gadolinium-activated glasses they are melted in a reducing atmosphere. With the aluminosilicate glasses described, this treatment leaves the europium impurity divalent, and it produces a blue luminescence. This appears to be a very sensitive test for europium. It is the absorption of the divalent europium ion which is believed to be harmful to gadolinium emission. Since it does not appear that gadolinium oxide much purer with respect to europium is likely to be obtained, a study of the effect of glass composition upon the europium luminescence has been initiated.

It has been found that the aluminosilicate glasses favor the maintenance of europium as a divalent. While air-melted gadolinium activated glasses do not show the blue luminescence of the divalent europium ion impurity, glasses containing higher proportions of euoropium show a purple luminescence composed of the blue emission of Eu^{2+} and the red emission of Eu^{3+}. Moreover, air-melting of alumino-silicate glasses produces a high ultraviolet base glass absoprtion, and hence this procedure cannot be regarded as the solution of the problem. Glasses free of aluminum seem to favor the formation of Eu^{3+} and therefore seem to be better prospects of reducing the interference due to Eu^{2+} impurity.

Neither the lithium-magnesium nor lithium-clacium glasses previously described could be prepared as stable glasses without high proportions of aluminum, but both soda-lime and barium crown glasses can. When either of these latter glasses activated by gadolinium is melted in a reducing atmosphere, no blue luminescence due to divalent europium is observed. Since the soda-lime glass appears to be more easily prepared in fair quality in our laboratory, attention is now being devoted to fabrication of a sample of this glass in suitable size.

The above study provides guide lines for the preparation of an efficient glass activated by trivalent europium. While both the soda-lime and barium crown glasses favor the oxidation of europium to Eu^{3+}, to date the soda-lime glasses have provided much more efficiently luminescing samples than have the barium crowns.

Although these Eu^{3+} glasses are excited by ultraviolet light down to at least 2500A, a portion of this excitation spectrum lies in the region of high ultraviolet absorption of air-melted silicate glasses. Soda-lime glass, like the alumino-silicate glasses, has a high ultraviolet transparency only when melted in a reducing atmosphere. While this effect is generally ascribed to reduction of trace impurities such as iron, it has been typical of glasses made from the purest raw materials prepared in our laboratory. The only solution to the above problem would be to devise silicate glass compositions in which the europium is not reduced by melting under reducing conditions, or to turn to borate or phosphate glasses which have better ultraviolet transparency when melted in air.

The work on gadolinium-activated glasses will be continued along the lines described, in an effort to provide improved materials. Principal attention will first be given to soda-lime glasses in an effort to obtain a composition which optimizes glass quality, freedom from radiation damage, and freedom from europium interference. A batch of the optimum composition will be prepared in about 100g. size in order to provide laser rods of more favorable geometry than those previously tested.

The work with europium-activated glasses will be continued. The first composition studied will be of soda lime glass, and an investigation of the effect of the melting atmosphere upon the base glass absorption as well as the europium valence state will be made. An effort to obtain an optimum composition for testing laser rods will be made. Some work on the properties of europium-activated borate and phosphate glasses will be started in order to determine the possibility of obtaining efficient glass phosphors whtch have a minimum of base glass absorbtion.

The effect of addition of minor portions of other ions to both gadolinium and europium-activated glasses will be investigated. For both types of glasses the most important purpose of these additions is to provide sensitizers for the activator emission, but the possibility of employing a trace of cerium to minimize radiation damage will also be examined.

A minor effort will be made to examine the possibility of obtaining divalent rare earth ions in glass by gamma irradiation of trivalent activated samples. This is not a strong possibility, and has never been accomplished in oxide type compounds. However, the technique of irradiation, followed by selective annealing to remove radiation damage to the glass without affecting a reduced rare earth ion, is an interesting possibility.

7. Persistent Enhanced Ultraviolet Radiation from Double-Pulsed Flash Lamps. (Dielectrics Branch, Solid State Division; and Plasma Physics Branch, Radiation Division.)

Enhanced ultraviolet output from double-pulsed neon flashlamps was recently reported by Emmet and Schawlow[1]. Double pulsing permits the

[1] J. L. Emmet and A. L. Schawlow, Applied Physics Letters 2, 204, (1963)

flash lamp to be more energetically excited without physical destruction than is possible by using a single pulse. By this technique, a gas discharge is first generated in the lamp by application of a low voltage pulse from a large capacitor in series with an inductance which determines the time-constant for the rise time of the current. Near the crest of the slow pulse a higher voltage is switched onto the lamp from a smaller capacitor in a relatively low-inductance circuit by a triggered spark gap. In this way the instantaneous current flowing in the tube can be increased from 2000 amp/cm^2 to 2500 amp/cm^2.

Since the above-reported high ultraviolet intensities were anticipated to be of use in pumping gadolinium-activated glass, a double-pulsing apparatus was set up. The measurements of Emmet and Schawlow were extended to 2000A using a 500 mm focal length grating monochromator with a 935 photodiode detector. The flashlamp output in the 3300-3800A wavelength region was separately monitored using a 917 photodiode with a Corning 9863 glass filter. The ratio of the peak detector output during the fast pulse to the output during the slow pulse was monitored in the region from 2000 to 4000A and commercial U-shaped xenon flashlamps were used. The data of Emmet and Schawlow were qualitatively confirmed; furthermore, the measured peak ratio at 2000A was about three times that at 3000A.

However, there is a new effect associated with the time-history of the radiation which becomes important at wavelengths below 3000A. The wavelength dependence of this effect is shown in Figure 29 (A, B, C, and D). After the occurrence of the fast pulse, the radiation during the slow trace does not return to a continuation of the radiation during the slow pulse as does the lamp monitor, but continues at an enhanced value as long as current flows through the lamp. A corresponding enhancement of the flashlamp current is not observed. The persistent enhanced ultraviolet radiation does not occur if either the fast pulse or slow pulse is applied to the lamp individually. This effect (exclusive of enhancement <u>during</u> the fast pulse) amounts to an integrated radiation increase of about <u>twice</u> that of the slow pulse at 3000A, and about a factor of twenty at 2500A. In Fig. 29 (E and F) it is shown that the enhancement effect can be made to persist during the entire slow pulse if the fast pulse occurs at the beginning of the slow pulse.

Another series of experiments was carried out at 2500A to see if the persistent ultraviolet radiation enhancement depended on the rate of energy delivery to the plasma. Inductors of several different values (570, 285, 80, 30, and 15 μh) were placed in series between the fast bank and the lamp. It was found that the enhancement depended strongly upon the value of inductance used. Essentially, the effect was not observed with an inductance greater than 100 μh, but a persistent enhancement of about one half that of the "no inductance" value was attained using an inductor of 30 μh. Experiments were carried out in which an ignitron tube was used to short out the flashlamp about 100 μ sec after the fast pulse; the 2500A photosignal was then observed to decrease greatly. This shows that the persistent enhanced output is associated with current flow through the lamp.

Similar temporal behavior of the ultraviolet radiation output of U-shaped, double-pulsed flashlamps filled with 300 mm Hg of argon was also observed.

The single and double pulse spectra of xenon and argon U-shaped flashlamps were recorded photographically using a Hilger medium quartz spectrograph. Sample spectra are shown in Figure 30. The argon (Fig. 30A) and xenon (Fig. 30B) exposures were made under approximately the same double-pulsing conditions. A noteworthy feature is the intense line spectrum in the ultraviolet which is <u>common to both</u> flashlamps. These lines are too intense to be merely a <u>common impurity</u> in both gases. Fig. 30D shows the spectrum of an argon lamp with slow pulse excitation only; Fig. 30C shows the spectrum of the lamp with fast pulse excitation only. It will be noticed that in both of these spectra the intense ultraviolet emission lines in Fig. 30A and 30B do not appear, although many of these same lines are observed in absorption in Fig. 30C. Figs. 30E and 30F show the double-pulse spectra of this lamp; in Fig. 30F the slow pulse comes first, followed by the fast pulse near its crest. In Fig. 30E, the fast pulse is initiated simultaneously with the slow pulse. The continuous spectrum in Fig. 30F (slow-fast) is stronger than that in Fig. 30E, (fast-slow), whereas just the reverse is the case for the line spectra. Hence it appears that the relative intensity of line emission to continuous emission can be controlled somewhat by varying the delay time of the fast pulse.

Almost all of the ultraviolet lines resulting from the double pulsing can be identified as neutral silicon (SiI) lines. Many of these lines are also observed in double-pulsed mercury flash lamps. It is roughly estimated from the photoelectric measurements that the peak persistent enhanced signal in the silicon lined (15A bandwidth) at 2881A corresponds to a lamp output of about 50 watts. Further measurements show that the persistent radiation is primarily associated with the line spectrum rather than the continuum.

The mechanism by which this persistent enhanced ultraviolet radiation occurs may be inferred from the present data. It appears that the fast pulse vaporizes the silicon in the fused silica walls of the lamp. The excitation threshold of the SiI spectrum is low enough so that the radiation can be maintained for the duration of the slow pulse. It is noted that the SiI spectrum is seen in absorption with only the fast pulse not only in xenon and argon flashtubes (Fig. 30C) but also in mercury flashtubes. This also has been previously observed (NRL Memorandum Report 1442) in the spectra from exploding wires in vacuo, where fused silica vacuum walls are used. This demonstrates that the fast current pulse produces silicon in the discharge, and that the slow current pulse is required to convert the absorption spectrum to emission spectrum.

From the relative intensities of the lines to the usual argon or xenon continuum in Figs. 30E and 30F, it appears that, due to the silicon produced in the discharge by the fast pulse, a large fraction of the ultraviolet radiation is emitted by the silicon rather than by the gas used to fill the lamp. This persistent enhanced ultraviolet output below 3000A may be useful for optically exciting luminescent ions with long spontaneous emission lifetimes. Of course, the enhanced ultraviolet output at longer wavelengths during the fast pulse is also available for ultraviolet-excited activators with both long and short lifetimes as suggested by Emmet and Schawlow. The appearance of intense silicon emission lines in the spectra of double-pulsed flashlamps suggests the possibility of obtaining similar enhanced radiation at different wavelengths by applying a thin coating containing the source of the desired radiation to the inside wall of the flashlamp.

8. Pumping with Light from Exploding Wires. (Analysis and Theory Branch, Radiation Division).

An experimental study was made of the relative efficiency of the optical coupling used between the exploding wire and the cylindrical rod being pumped. (cf. Fig. 9, NRL Memorandum Report 1442). The optical efficiency of the right elliptical cylinder as a reflector was studied using a PEK xenon lamp as the light source and a ruby laser, driven just to threshold, as a means of testing the relative optical coupling efficiency.

It was found that an aluminized mylar material with a mirror finish was better than the bright but relatively diffuse aluminum tape which had previously been used for the reflecting surface. (It is necessary that a replaceable surface be used in this explosion chamber since the quartz tubing around the wire shatters during the more energetic shots and damages the reflecting surface). It was found that the addition of a top reflecting plane lowered the necessary light output to produce ruby threshold by a factor of approximately 2. Adding a second reflecting plane to the bottom further lowered the necessary light by another factor of 1.5.

The top reflecting plane could easily be used in exploding wire shots, because the surface to which it is attached is brass and has no high voltage gradients during the shot. Use of the reflector on the bottom surface presents problems, however, because voltages of about 250 KV are applied to the wire. Since all broad band high efficiency reflectors are conductors, attempts to use a metallic bottom reflector have not yet been successful, because the discharge breaks over to the reflector rather than going through the wire. In recent weeks we have tried a surface of demineralized water on top of the bottom nylon insulating surface, without breakdown up to about 230 KV. The reflecting efficiency of this water surface has not yet been measured.

The optical studies also revealed that the molded epoxy right elliptical cylinder being used did not focus as well as was desired. A machined aluminum cylinder was therefore fabricated. For the reason previously stated this reflector is also lined with aluminized mylar (0.005" thick). The improvement in optical focusing is shown in Fig. 31.

Attempts were made to increase the optical input to the laser rod from the exploding wire. An optical detector probe was made, consisting of a 1P28 photomultiplier looking at the end of a 7 mm diameter quartz rod which is placed in the laser rod position of the ellipse. Thus the detector measures the relative amount of light focused on the rod. Several experiments were performed with this arrangement.

The 17 mm evacuated tube around the wire was reduced to 7 mm in the hope that the plasma would be confined to a smaller diameter. Streak camera pictures showed that this was true, but the probe detector output with the 17 mm tube was higher.

The following arrangements were also tried without increasing the peak or integrated input to the probe, (a 2400-3200A bandpass filter was used in the probe for these measurements):

1) A 2 mm quartz tube was placed around the wire, both being inside the evacuated 17mm tube.

2) A 7 mm quartz tube was placed around the wire, both being inside the evacuated 17 mm tube.

3) The 17 mm tube was filled with water instead of being evacuated.

4) The size of the wire was changed from 0.003" to 0.001", 0.002", 0.004", and 0.005".

The wire when exploded in air at atmospheric pressure did give a somewhat greater peak detector output, but the shock wave broke the detector rod and this was considered impractical because of possible damage to the etalons under test.

The improved explosion chamber with the machined aluminum right elliptical cylinder was then mounted on the water capacitor and attempts were made to pump the ruby rod to threshold with the exploding wire, without success. This was somewhat surprising, since about 1300 joules can be stored in the water capacitor and discharged into the exploding wire and the series water switch, without apparent breakdowns around the wire (the division of energy between the wire and the series switch is not known). By contrast the previous experiments had shown that the ruby would lase when only 440 joules were discharged through the xenon lamp, even with the relatively poor epoxy right elliptical cylinder.

The wire and xenon lamp were then experimentally compared using the quartz rod detector probe described above. It was found that the time-integrated input to the rod from the exploding wire above 3650A (the short wavelength cutoff for the neutral density optical filter used) was about 2.7 times lower than that from the xenon lamp operated at a level corresponding to the ruby lasing threshold. The fact that the xenon light is confined to a 5 mm diameter for the entire output time is greatly in its favor. The peak light power from the wire (light energy/μ sec) was about 12 times that of the xenon lamp. With a 2400-3200A filter on the quartz rod detector, it was found that the time-integrated light in this range from the xenon lamp was about 1.6 times higher than that from the wire, and the peak output of the wire was about 45 times that of the xenon lamp.

The above results show that the ratio of time-integrated light in the 2400-3200A range to that above 3650A is greater for the exploding wire than for the xenon lamp by a factor of about 2. It is likely that if the ultraviolet range extended down to 2000A, the ratio would be even higher.

In view of this possibility and of the enhanced ultraviolet absorption of ruby found in the NRL Report 1442 (pp. 2-4, and Figs. 1-5) it was decided to study the effect, on ruby pumping, of filtering out the ultraviolet wire output below Pyrex cutoff. The ruby laser rod was pumped with several exploding wire shots, half with the wire inside an evacuated quartz tube and half inside an evacuated Pyrex tube. The level of ruby detecting the R_1 and R_2 fluorescence lines. The ruby was not pumped to threshold. The detector was a spectrograph looking at one end of the ruby through a tube, with an RCA 7265 photomultiplier at the film surface covering a band of about 150A centered about the R_1 and R_2 lines. The results are shown in Fig. 32. There is considerable fluctuation from shot to shot, so that clear-cut conclusions are not possible. It appears, however, that the inclusion of the ultraviolet below Pyrex cutoff seems to have no overall effect on the pumping efficiency.

It is planned to use argon and perhaps xenon filled tubes as loads for the fast water capacitor to see if higher peak values of ultraviolet output can be attained. The double-pulsing technique described elsewhere in this report will also be tried, using the water capacitor to deliver the intense short pulse.

Attempts to excite a $LiMgAlSiO_3$ glass etalon containing 0.001 cationic mole fraction cerium were again made, with the more efficient optical coupling system described above. The fluorescent output of the etalon was stronger than before, but as yet no evidence of stimulated emission has been obtained. Etalons with 0.00003, 0.0001, and 0.0003 cationic mole fraction cerium are being fabricated in the Solid State Division for further tests.

9. Fundamental Investigation of Pumping Light Sources. (Plasma Physics Branch, Radiation Division)

The radiation from plasmas has received continuing attention in the Plasma Physics Branch as light sources for laser excitation. During the past half year the activities have included the study of the radiation from pulsed arc-type discharges and the technical problems encountered at high energies, as well as the theoretical radiation calculations and operation of the θ-pinch facility which were described in NRL Memorandum Report 1442.

(a) Radiation from Pulsed Arc Discharges.

The state of the art of operating pulsed arc discharges at relatively high pressure (100 to 500 Torr) has been critically reviewed. A major uncertainty concerning the use of such light sources at high power is the unknown spectral distribution of the radiation and its dependence on the tube and power supply parameters. Published investigations of the spectral distribution of conventional flashlamps have concentrated on the visible and infrared regions of the spectrum with tubes operated at rather modest power levels (less than 100 kW/cm^3). Furthermore the effects of tube parameters such as pressure and diameter have not been reported; often even the values of these parameters are not reported. It is known that as the input power is increased the spectral region of greatest intensity shifts toward shorter wavelengths. The extent of this shift in wavelength and intensity and how tube parameters can be varied to maximize the intensity at a particular wavelength, are the subjects of current investigations here.

It has been found that the relatively low intensity of a tungsten lamp makes it an unsatisfactory spectrograph-calibration standard for working with the high intensities and low wavelengths encountered, and a carbon-arc calibration standard is presently being set up for use in making absolute measurements of the spectral distribution from various light sources.

(b) Technical aspects of high power flashlamp operation.

A second major uncertainty concerning the operation of flashlamps at very high power is what can be done to circumvent the mechanisms for electrode erosion and tube fracture which severely reduce the tube life. Furthermore, at high voltages, cathode material is sputtered off by the impacting ions. This material is deposited on the walls of the lamp and reduces its brightness. A self cleaning lamp, i.e., one in which the walls remain hot enough to re-evaporate the material onto some cooler part of the lamp body, would be desirable. Flashlamps with rugged connections and thick walls are being prepared to investigate materials limitation with high current densities.

An electrical shock tube operating at relatively high pressure (10-50 mm He) was used to produce intense light flashes amounting to 100 kW/cm^2/100 A band-width in the near UV. Two mechanisms of tube fracture have been noted.[1] Fractures due to the internal pressure pulses

[1] R. C. Elton, "Radiation Induced Shock Waves in Air External to Pharos Quartz Tubes", paper presented at annual Meeting Div. of Plasma Physics, Nov. 1963, San Diego, California; H. R. Griem, R. C. Elton, A. C. Kolb, W. H. Lupton, E. Hintz, Report of NRL Progress, Oct. 1963.

may be prevented by preheating with the double-pulsed circuit discussed in NRL Memorandum Report 1442 and in Item 7 of the present report. Fractures due to radiation-induced external pressure pulses have received intensive study because of their applicability to the 2-megajoule PHAROS θ-pinch experiment as well as the shock tube experiment mentioned above. This radiation is produced from silicon vaporized from the interior wall. Some of the strongest silicon lines lie in the region below 1900A which is transmitted by fused silica envelopes and is also in the region of strong absorption by oxygen and ozone. This radiation can be absorbed within 0.1 mm of air external to the tube, producing a hot layer and a resulting pressure pulse. The threshold for quartz breakage by this effect is observed to be 25 kW/cm^2-sr-100 A in a 7 μsec pulse for a typical 3 mm quartz tube. The tube destruction from this cause can be eliminated by removing the oxygen from the laser-flashlamp cavity.

(c) θ-pinch Facility.

The θ-pinch facility described in the previous progress report is now in operation. It is presently being used for a study of vacuum ultraviolet spectra in the region of 40 to 400 A. It is expected that other spectral regions will be investigated shortly when additional spectrographs are employed, and that a comprehensive picture of the behavior of this electrodeless discharge as a light source will emerge.

(d) Theory.

The operation of light sources at elevated temperatures ($\sim 10^5$°K or above) requires a knowledge of excitation and ionization rates in order to predict the spectral distribution of emitted radiation. This follows because there is usually insufficient time to establish Saha-Boltzman equilibrium and the solution of relevant rate equations is called for.

A computer program has been prepared since the last report in order to calculate the rate coefficients required for spectroscopic analysis. The program involves the numerical evaluation of collision rates for the various processes (excitation, ionization, recombination) which arise from electron-ion collisions. This program is now checked out and attention is presently being focused on a comparison of ionization rates, obtained from different theories, with existing experimental data.

The θ-pinch hydromagnetic-radiation computer code described in NRL Memorandum Report 1442 will be improved in the next months to take into account the resistivity due to the presence of high-Z ions and the additional pressure from stripped electrons.

10. Effects Due to High Intensity Laser Light. (Radiometry Branch, Optics Division).

In the course of setting up to resume experiments on the enhanced absorption in ruby two observations were made which are perhaps of sufficient interest to mention. One is the production of minute explosions when the output of a Q-switched ruby laser was brought to a focus under-water. The other is the excitation of green fluorescence in a water solution of fluorescein by the focussed output of a Q-switched ruby laser. Although the fluorescein was intended as a detector of coherent second harmonic radiation, indications were that the laser light was exciting the fluorescein directly by a two photon process.

Publications, Reports and Talks

1. Optical Absorption in Gd-Activated Glass, H. Gandy and J. Weller, Report of NRL Progress, October, 1963.

2. Persistent Enhanced UV Radiation from Double-Pulsed Flashlamps. H. Gandy, A. Kolb, W. Lupton and J. Weller, Report of NRL Progress, to be published. (Also submitted Applied Physics Letters)

3. "Light Sources for Laser Excitation", W. Lupton, H. Gandy, A. Kolb, and R. Elton, presented at First Conference on Laser Technology, San Diego, California, November (1963) and to be published in the Proceedings of this Conference.

Roster of Personnel and NRL Problem Numbers

The professional staff engaged in the research described above, and the applicable NRL Problem Numbers, are listed below.

Code 6440 (Dielectrics Branch, Solid State Division)
NRL Problem No. 64P03-04
H. W. Gandy*
R. J. Ginther*
J. Weller
J. H. Schulman

Code 7310 (Radiometry Branch, Optics Division)
NRL Problem No. 73N01-09
J. W. Tucker*
J. N. Bradford
L. Drummeter

Code 7410 (Analyses and Theory Branch, Radiation Division)
NRL Problem No. 74H03-21
J. Shipman*

Code 7470 (Plasma Physics Branch, Radiation Division)
NRL Problem No. 74H01-11
A. C. Kolb
W. H. Lupton*

The asterisks indicate the staff members who have prepared portions of this report.

Report submitted by

J H Schulman

19 December 1963 J. H. Schulman

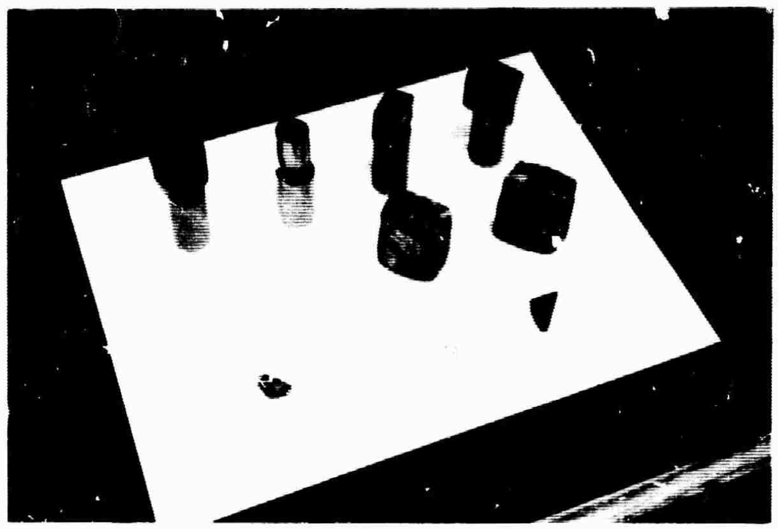

Fig. 1 - Ruby Samples Submitted by ONR

Top row, left to right: Linde #1830-16, Linde #1739-18 Thermal Syndicate #636, Thermal Syndicate #621.

Middle row: Thermal Syndicate #636 boule, Thermal Syndicate #621 boule

Bottom row: Airtron flux grown crystal,

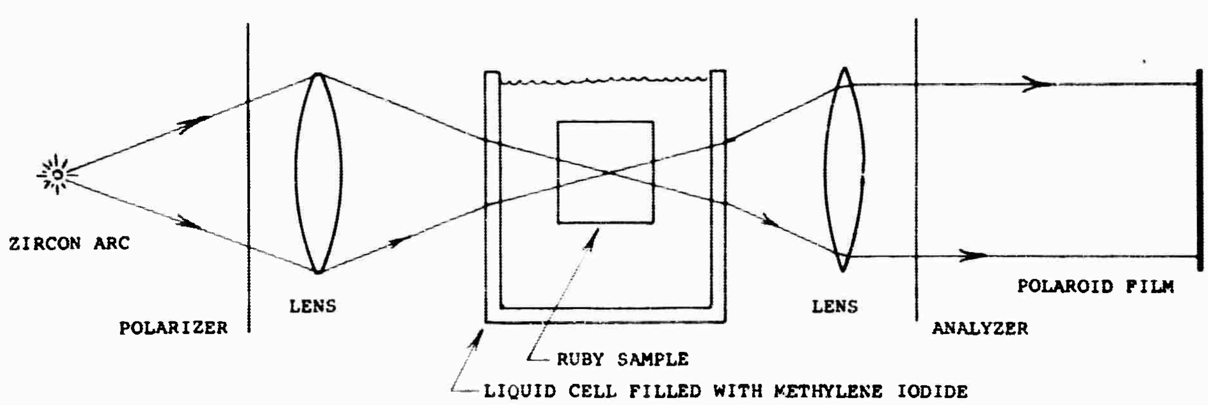

Figure 2 - Experimental Arrangement for Optic Axis Examination

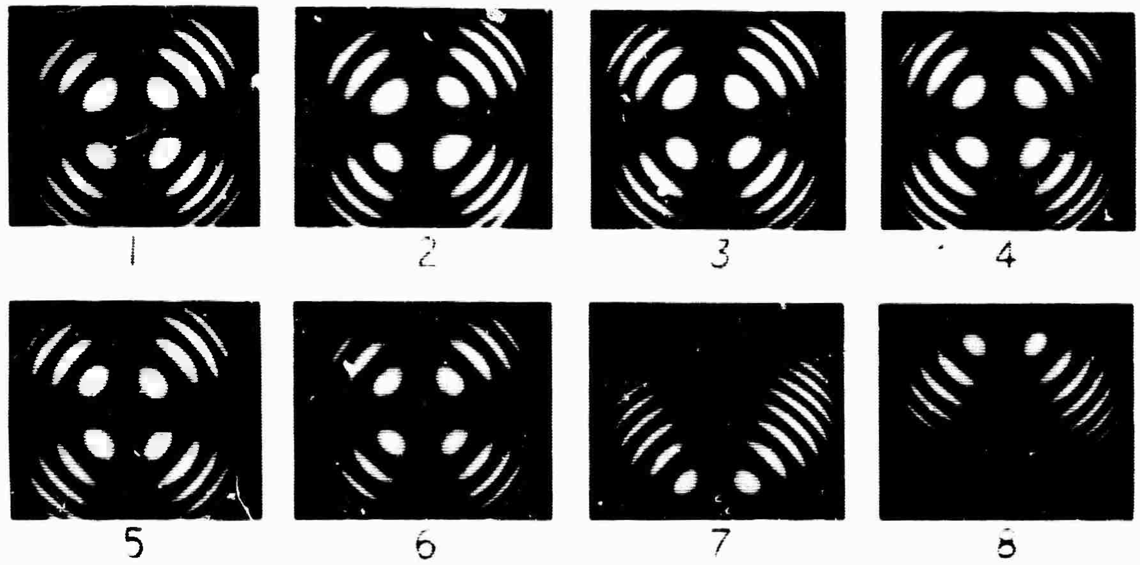

(A) Optic Axis Pattern
1-5 Different parts of the crystal viewed from the same direction
6-8 Same part of the crystal viewed from different directions

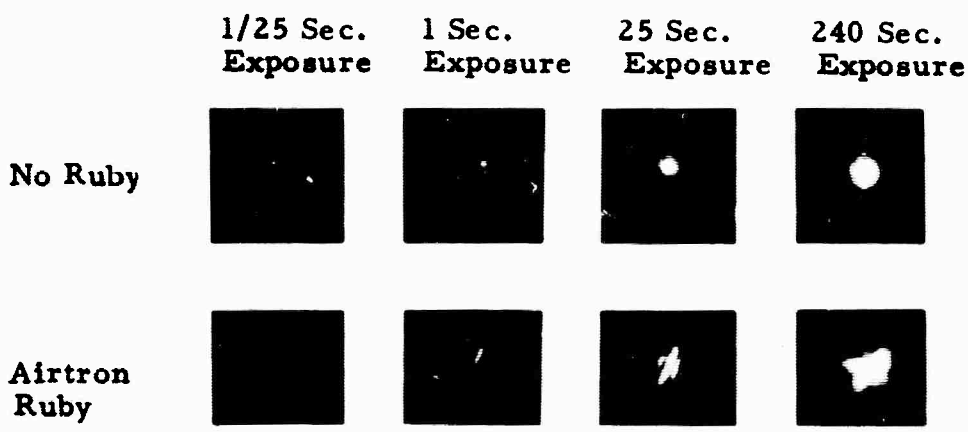

(B) Small Angle Scattering

(C) Strain pattern

Figure 3 - Optical Quality Studies of Airtron Ruby

Linde #1739-18

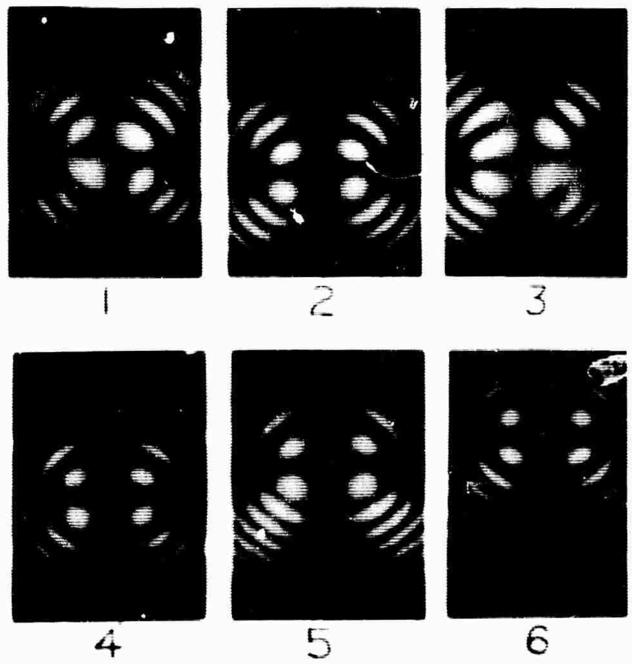

1-4. Different parts of the crystal viewed from the same direction
5, 6. Same part of the crystal viewed from different directions

Linde #1830-16

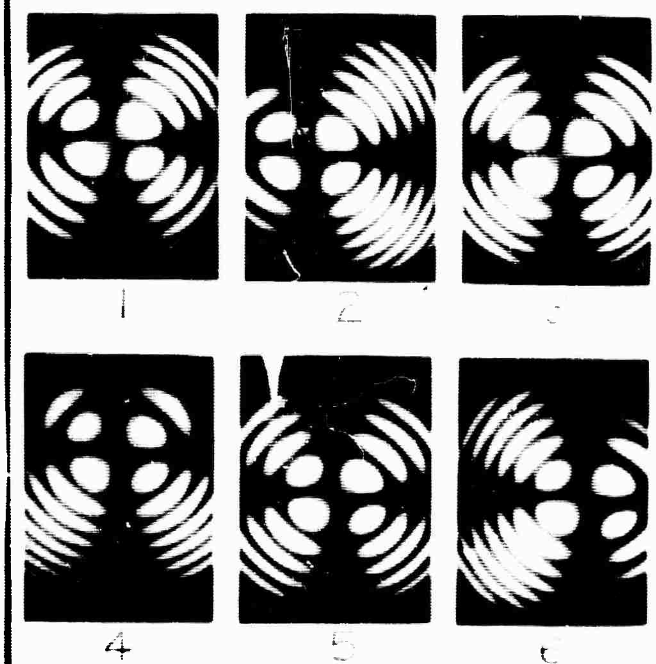

1-6. Same part of the crystal viewed from different directions

Thermal Syndicate #621

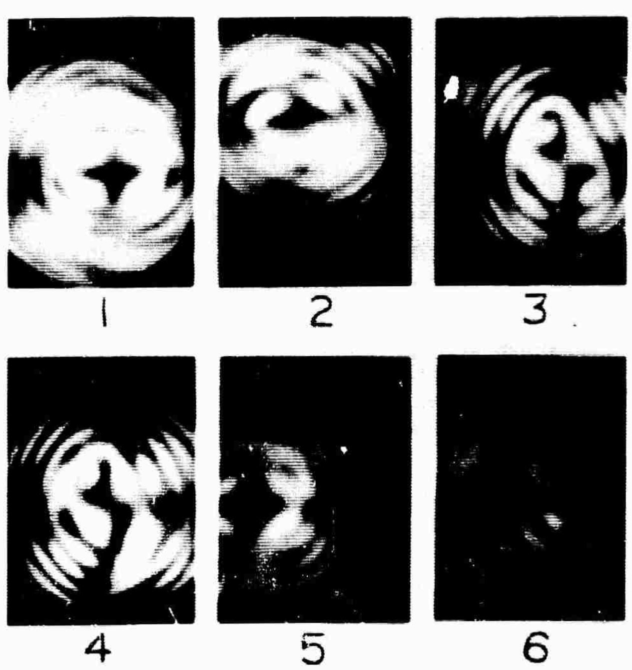

1-4. Different parts of the crystal viewed from the same direction
5, 6. Same part of the crystal viewed from different directions

Thermal Syndicate #636

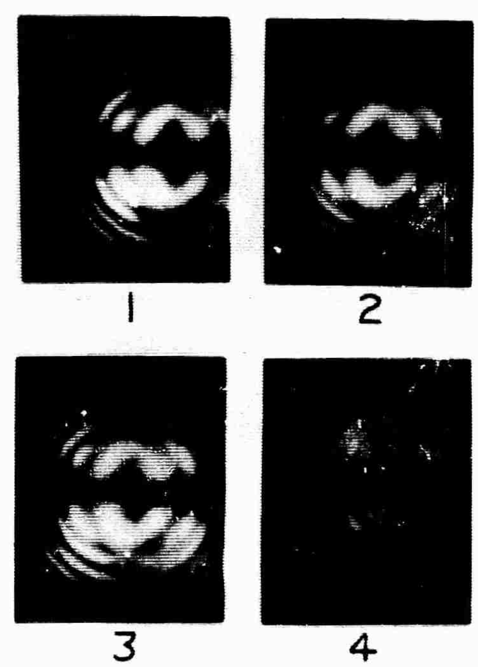

1-4. Same part of the crystal viewed from different directions

Figure 4 - Optic Axis Patterns of Linde and Thermal Syndicate Rub

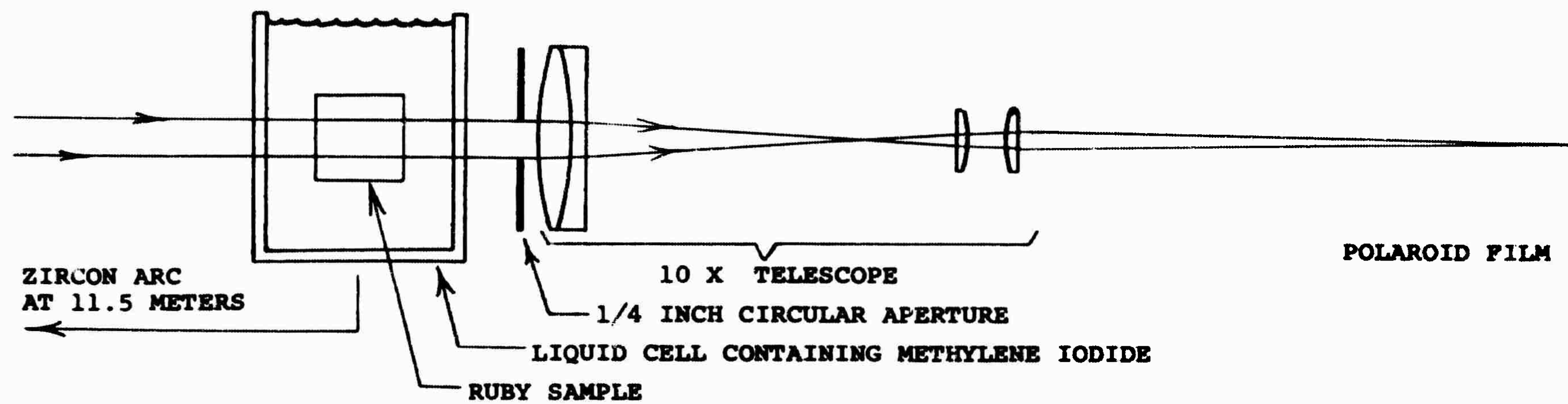

Figure 5 - Experimental Arrangement for Measurement of Small Angle Scattering

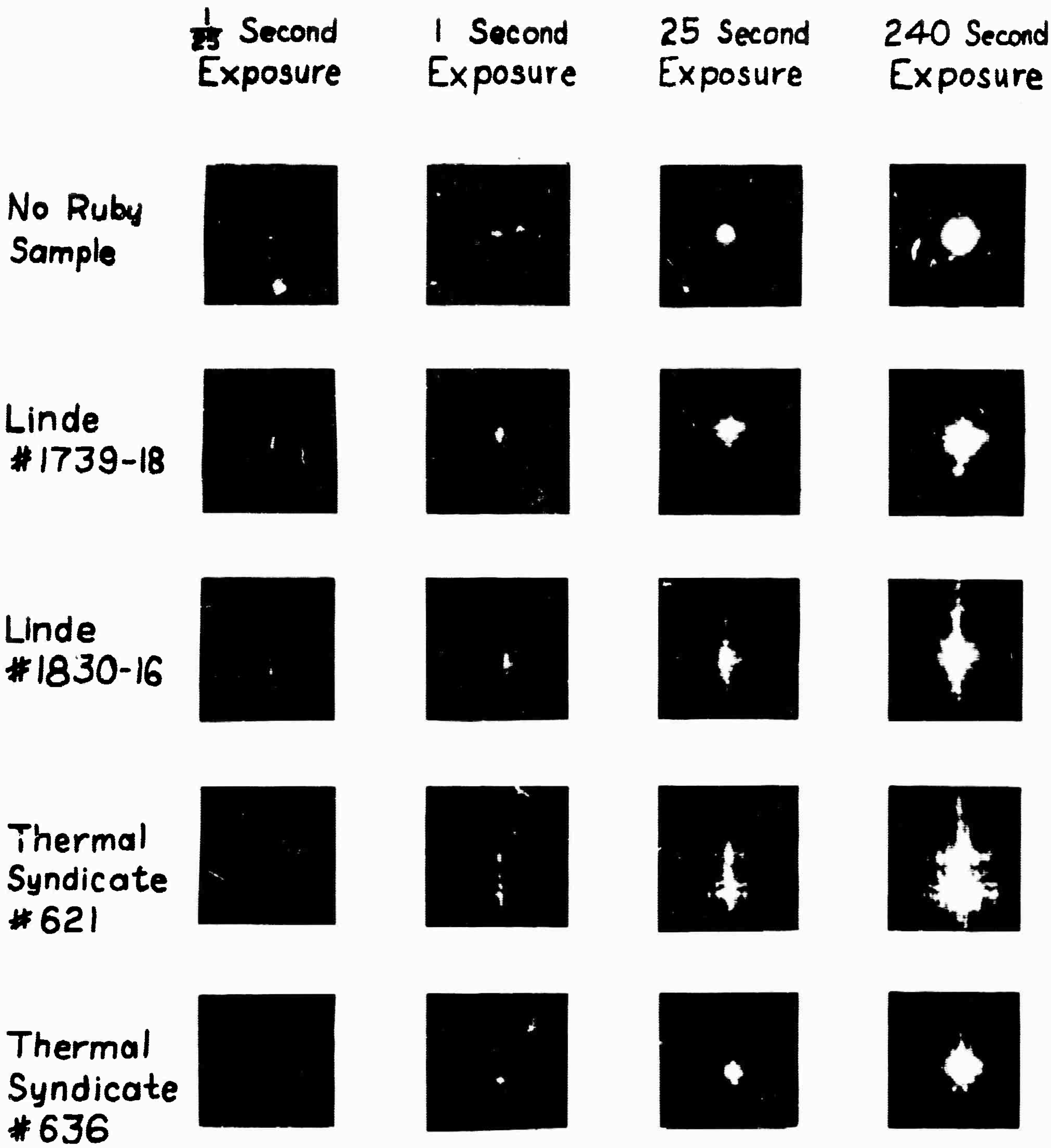

Figure 6 - Small Angle Scattering from Linde and Thermal Syndicate Ruby Boules

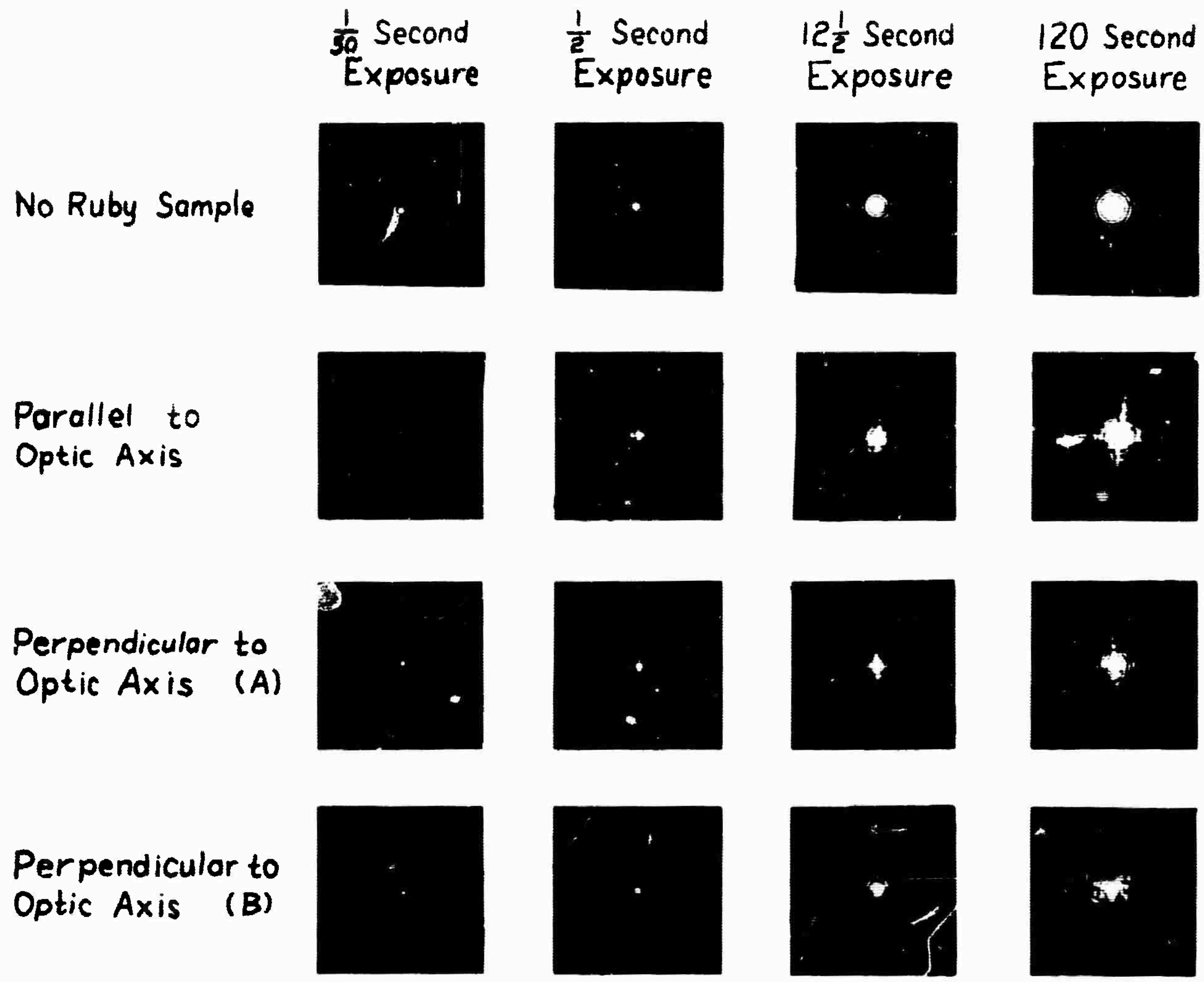

(A) Perpendicular to direction in which boule was drawn

(B) Parallel to direction in which boule was drawn

Figure 7 - Small Angle Scattering from Finished Thermal Syndicate #636 Ruby

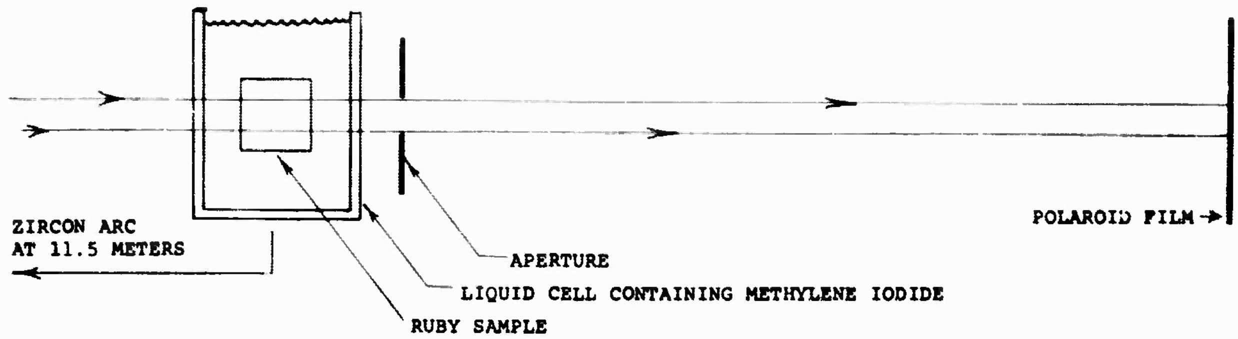

Figure 8 - Arrangement for Shadowgraph Examination

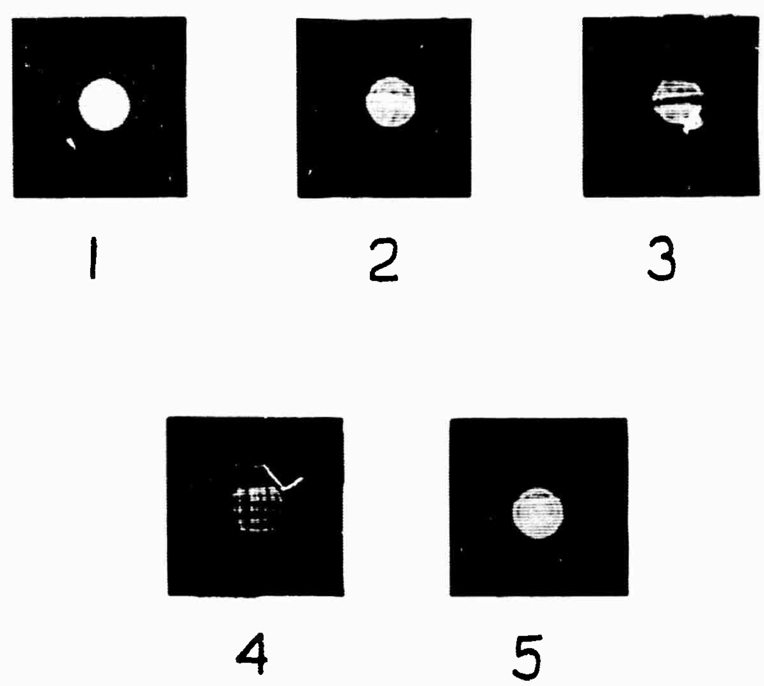

1. No ruby sample
2. Linde #1739-18
3. Linde #1830-16
4. Thermal Syndicate #621
5. Thermal Syndicate #636

Film placed 33-1/2 inches behind ruby sample

Figure 9 - Shadowgraphs of Unfinished Ruby Samples

(A) SHADOWGRAPHS MADE WITH OPTIC AXIS PARALLEL TO BEAM

a. Film 7 inches from crystal b. Film 33½ inches from crystal c. Film 7 inches from crystal, methylene iodide and cover glasses on surfaces

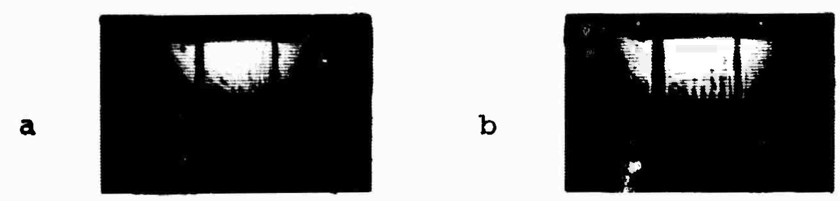

(B) SHADOWGRAPHS MADE WITH OPTIC AXIS AND DIRECTION IN WHICH BOULE WAS DRAWN PERPENDICULAR TO BEAM

a. Film 7 inches from crystal b. Film 33½ inches from crystal

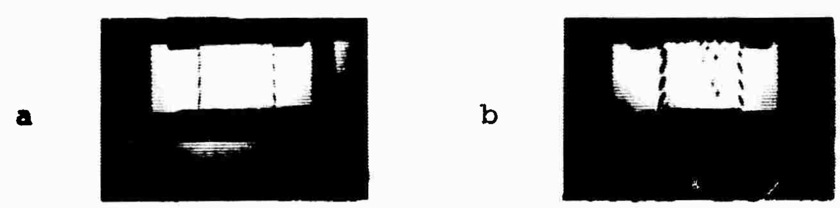

(C) SHADOWGRAPHS MADE WITH OPTIC AXIS PERPENDICULAR AND DIRECTION IN WHICH BOULE WAS DRAWN PARALLEL TO BEAM

a. Film 7 inches from crystal b. Film 33½ inches from crystal

(D) EXAMINATION BETWEEN CROSSED POLAROIDS

a. Parallel to optic axis ($\frac{1}{50}$ sec.) b. Perpendicular to optic axis and direction boule was drawn (½ sec.) c. Third orthogonal direction (5 sec.)

Figure 10 - Shadowgraphs of Finished Thermal Syndicate #636 Ruby

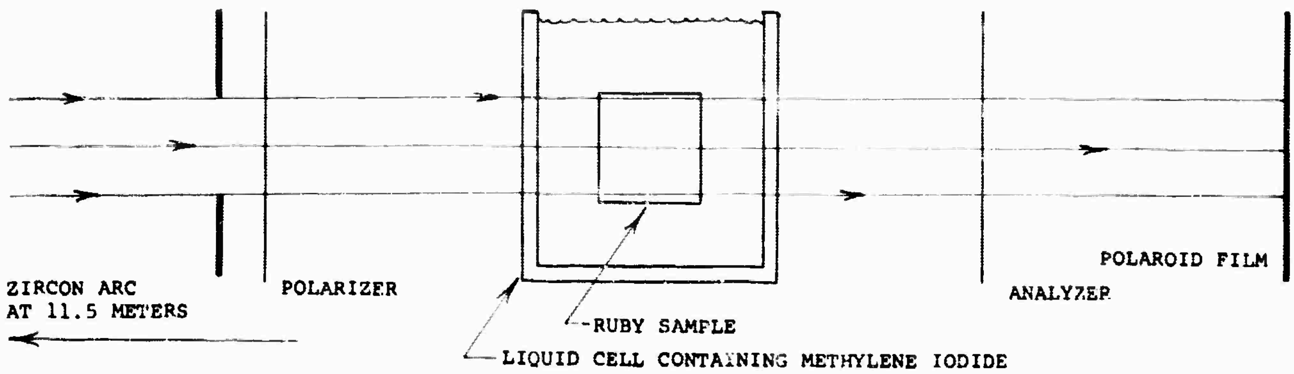

Figure 11 - Experimental Arrangement for Crossed Polaroid Examination

Linde #1739-18

Linde #1830-16

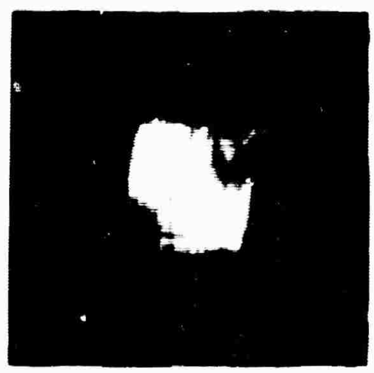

T.S. #621

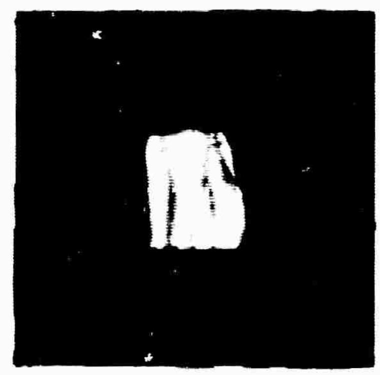

T.S. #636

Figure 12 - Crossed Polaroid Patterns of Linde and Thermal Syndicate Boules

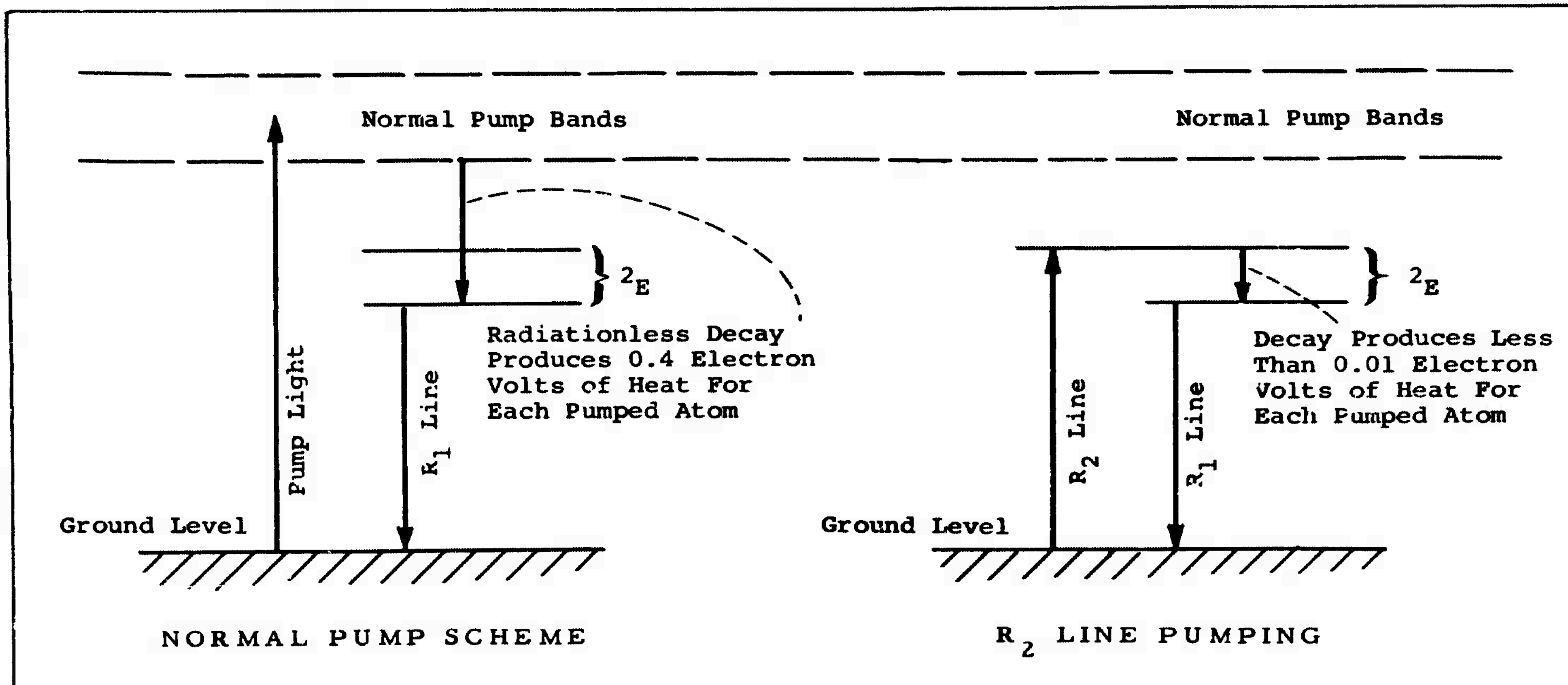

Figure 13 - Comparison of Normal Pumping of Ruby With Pumping by R_2 Lines (Schematic)

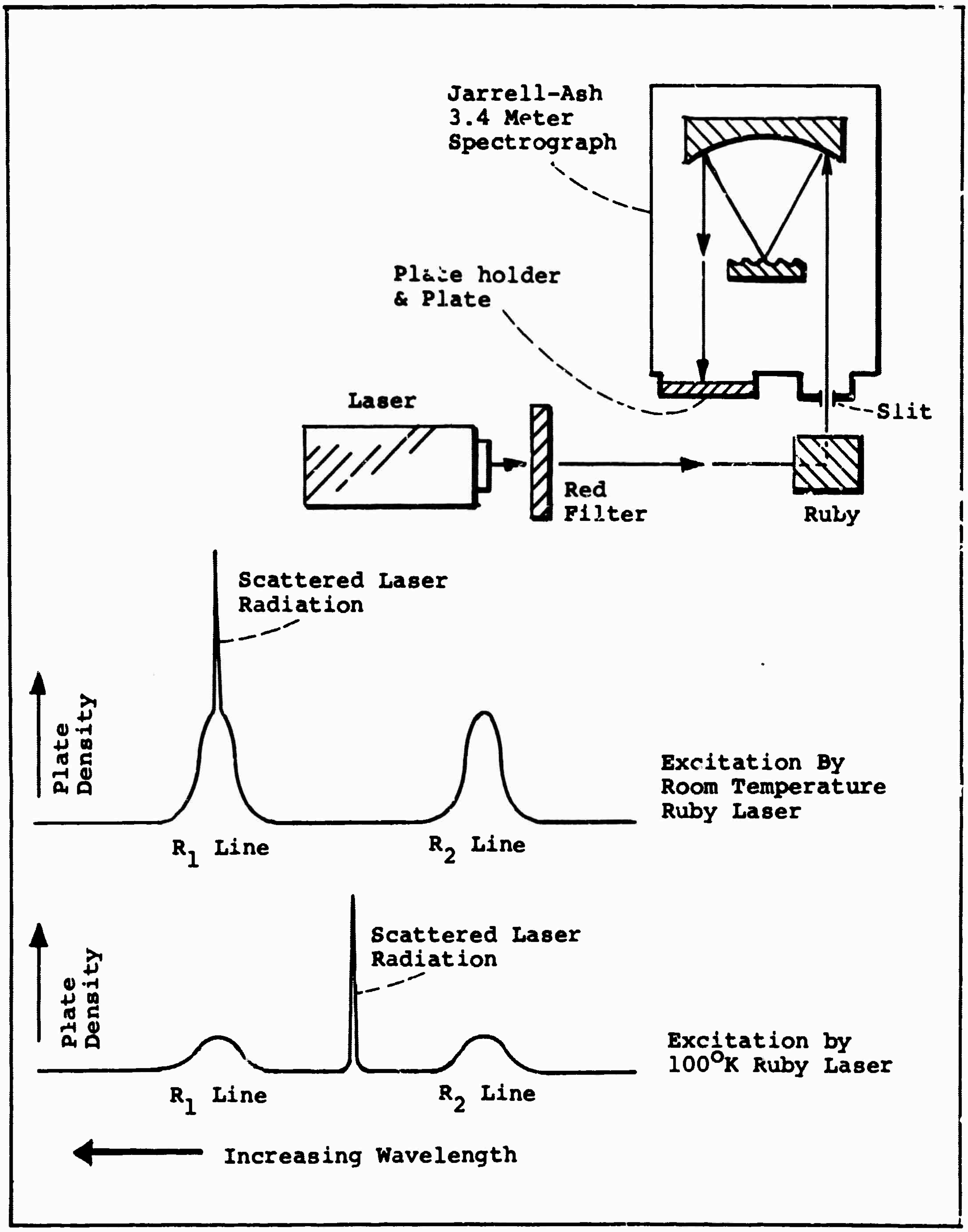

Figure 14 - Effect of Excitation Wavelength on R-Line Output

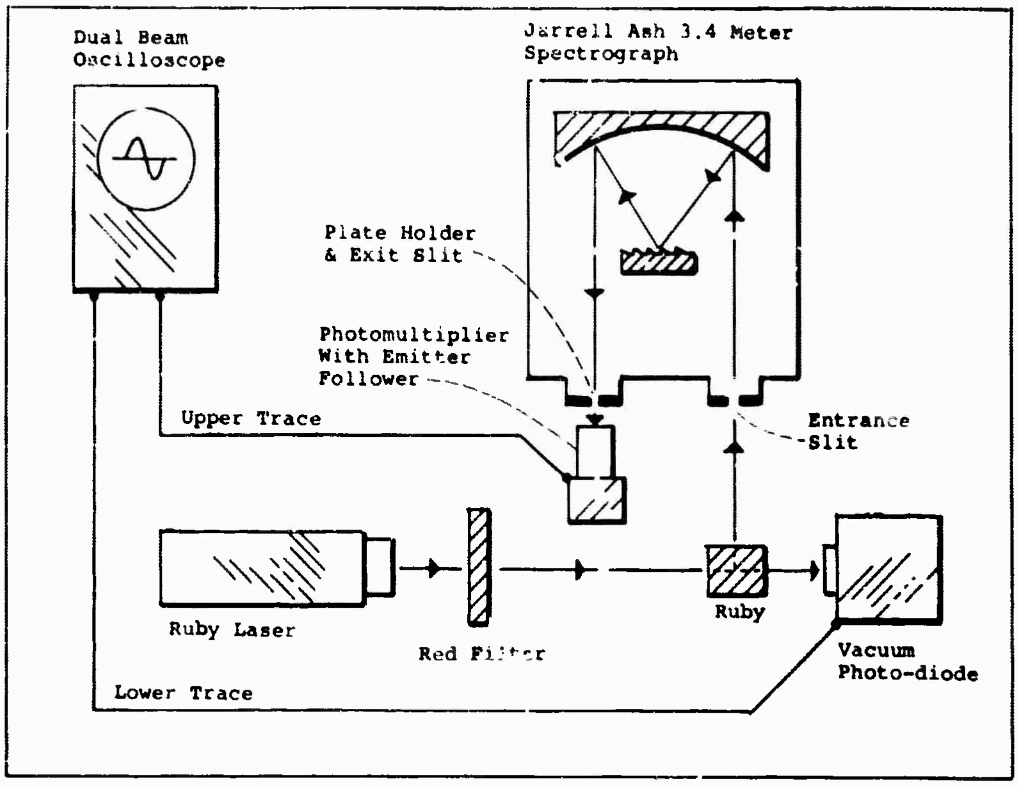

Figure 15 - Experimental Arrangement for Oscillographic Study of Filling of ^2E Level in Ruby

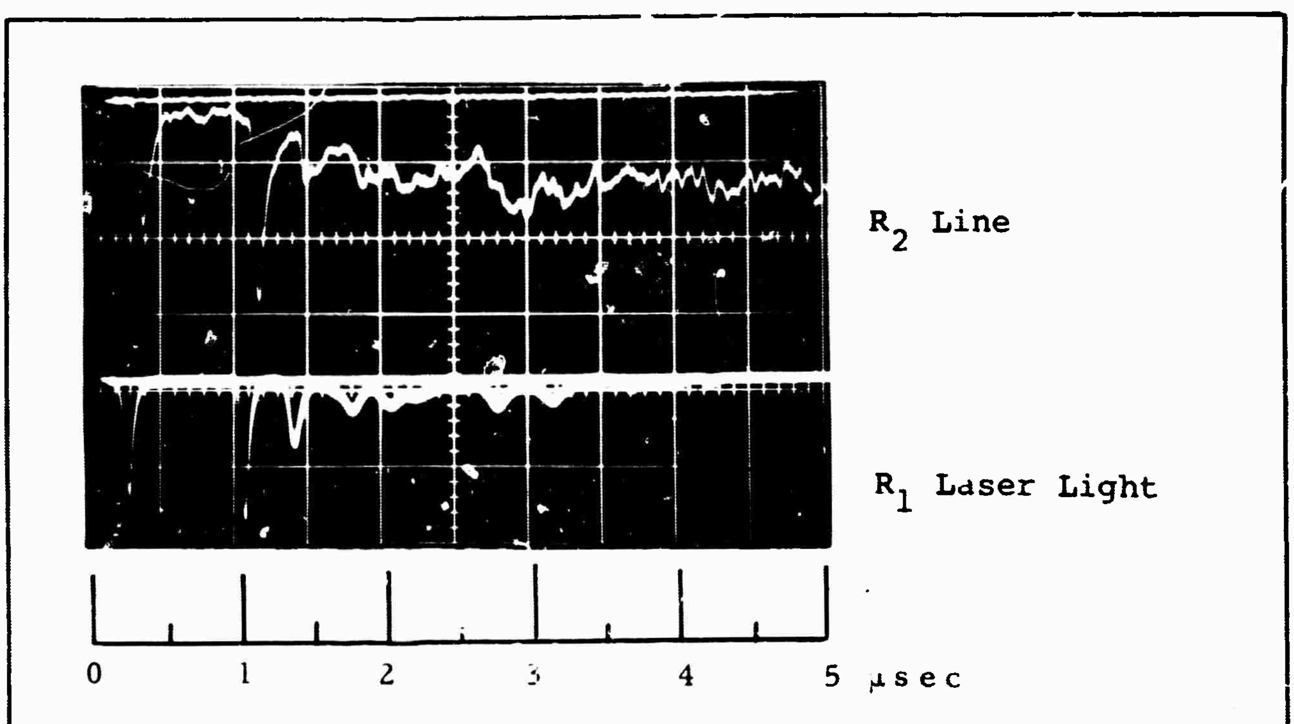

Figure 16 - Time Relation Between Exciting Radiation and Excited Pulses. The large spikes in the upper trace are from scattered laser light - their apparent delay is mainly due to photomultiplier transit time.

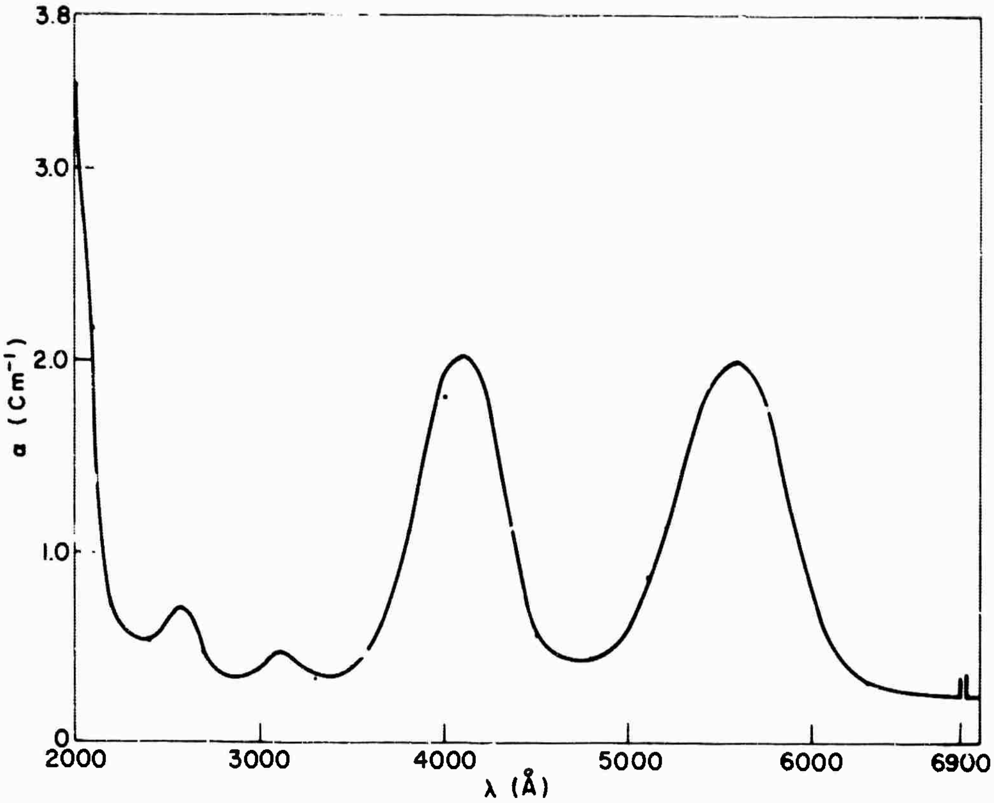

Figure 17 - Room Temperature Absorption Spectrum of Meller 0° Ruby Doped with 0.04% Chromium

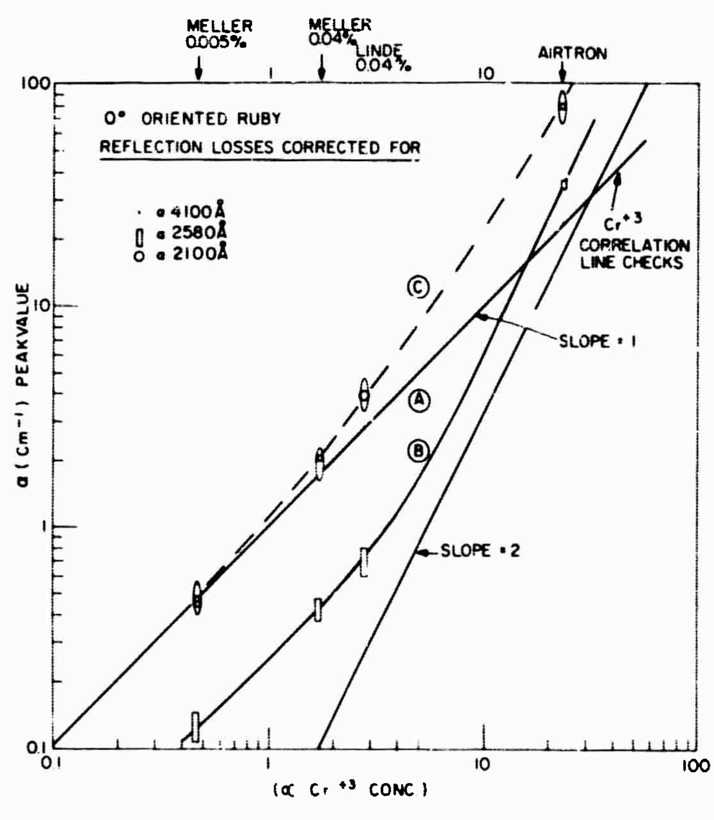

Figure 18 - Absorption Coefficients of Band Maxima vs Cr^{+3} Concentration

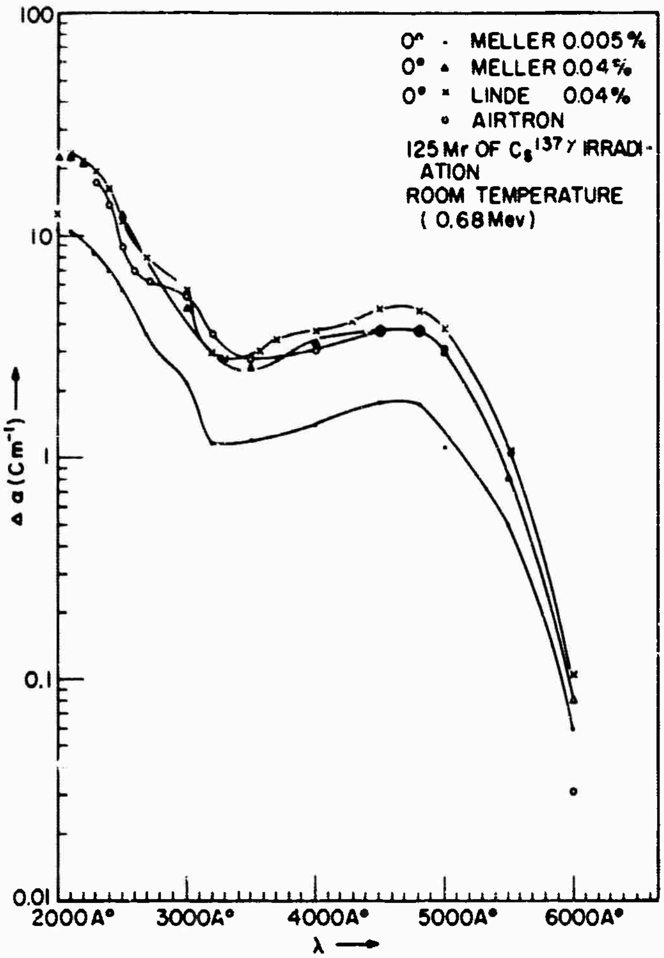

Figure 19 - Radiation-induced changes in Absorption Spectra of Various Rubies

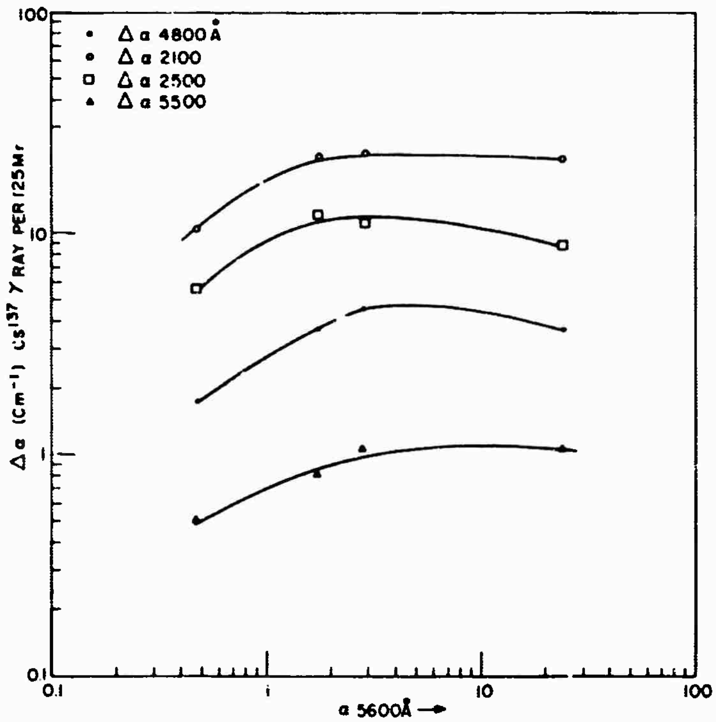

Figure 20 - Concentration-dependence of Radiation-induced Absorption in Ruby

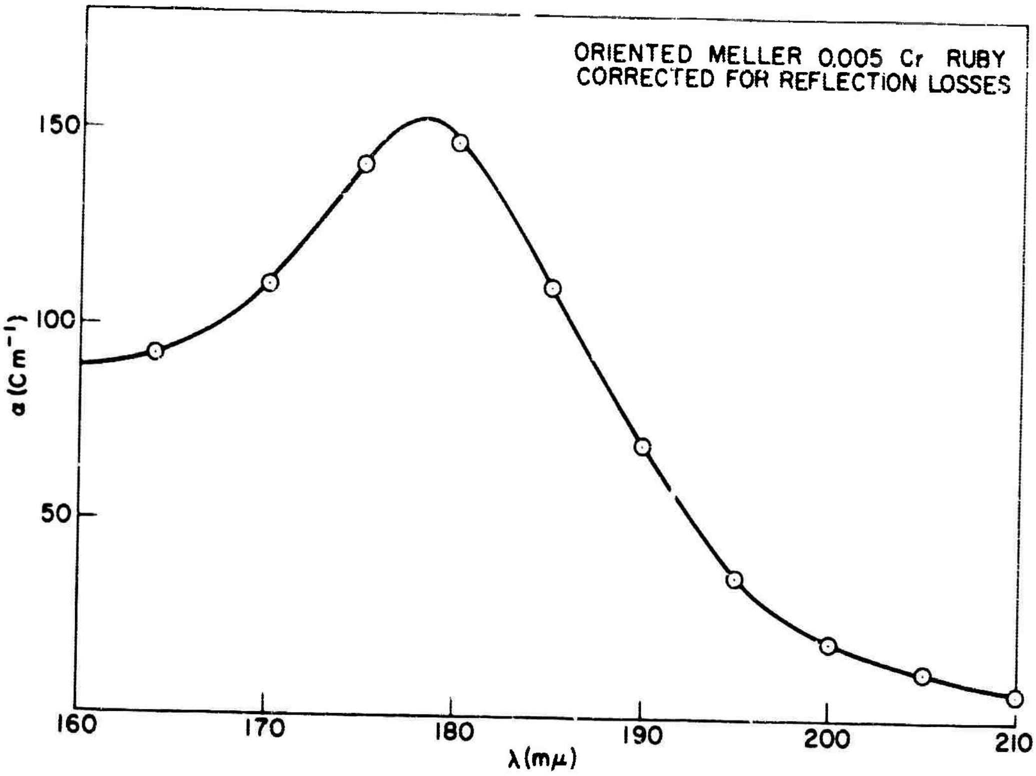

Figure 21 - Absorption Spectrum of Ruby in the Vacuum Ultraviolet

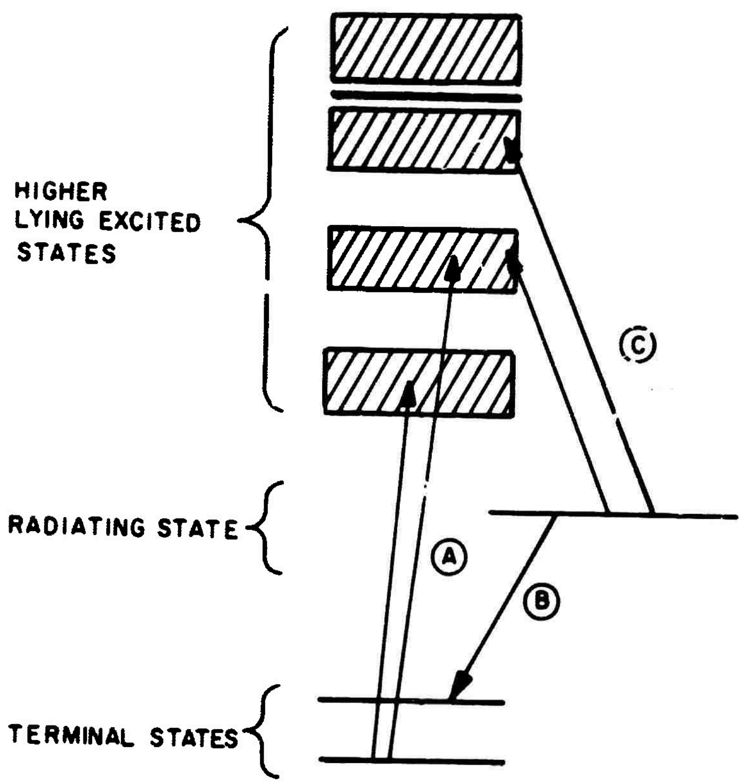

Figure 2? - Idealized Energy Level Diagram for Gadolinium-activated Glass

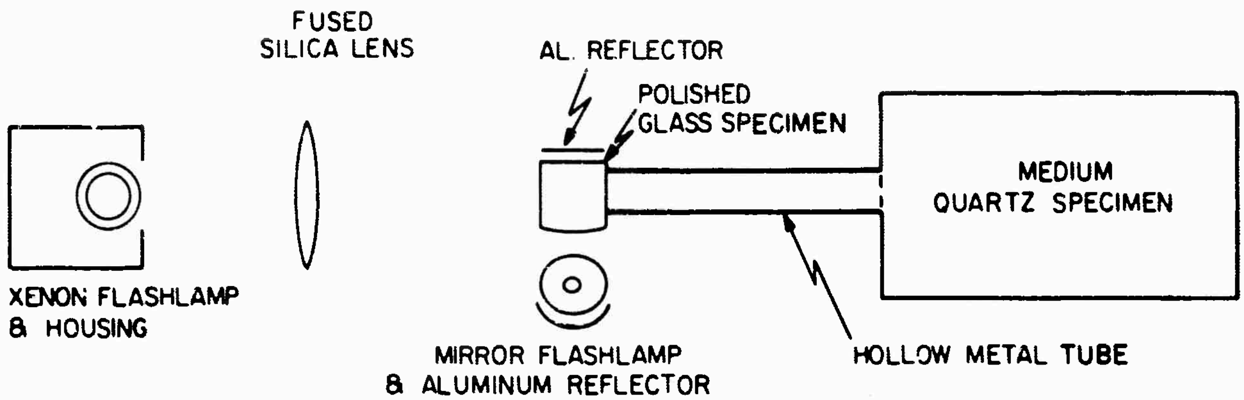

Figure 23 - Arrangement for study of Excited-state Absorption in Gadolinium-activated glass

(A)

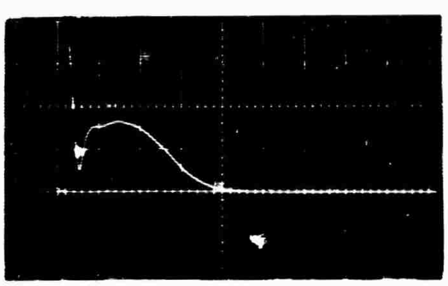

(B)

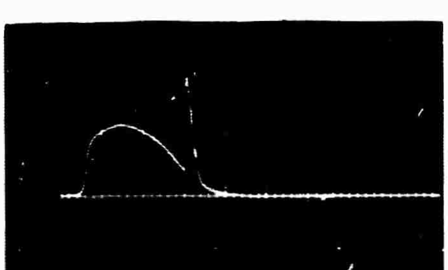

Figure 24 - Time Record of Light Intensity in Excited-state Absorption Experiments on Gadolinium-activated Glass. Writing Speed 500 μsec/cm.

(A) Xenon pulse first, followed by mercury excitation pulse.

(B) Mercury excitation pulse followed by xenon interrogation pulse.

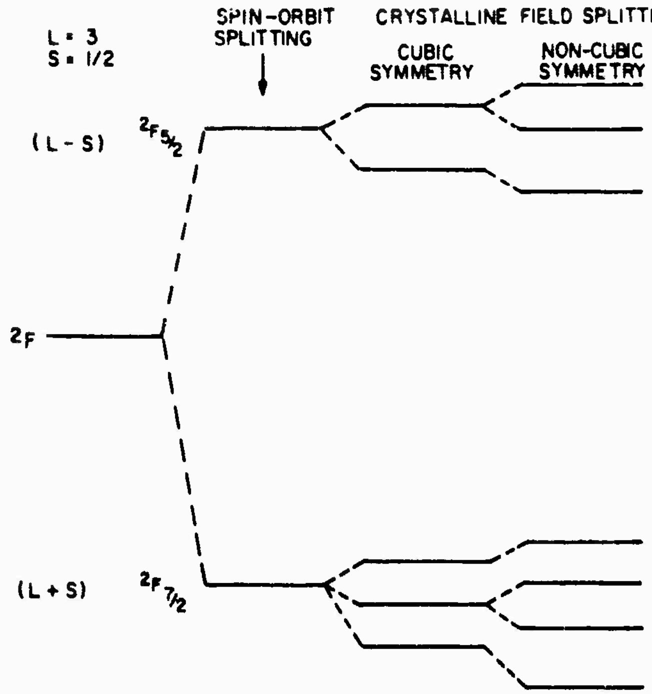

Figure 25 - Schematic Representation of ^{2}F Doublet for $Yb^{\pm 3}$ $4f^{13}$ Configuration with Orbital Degeneracy Removal by the Spin-Orbit Effect and the Crystalline Field of the Host Matrix.

Spin Orbit splitting is about 10,000 cm^{-1} ($\lambda \sim 1\mu$) and crystalline field splitting can be in the order of a few hundred cm^{-1}.

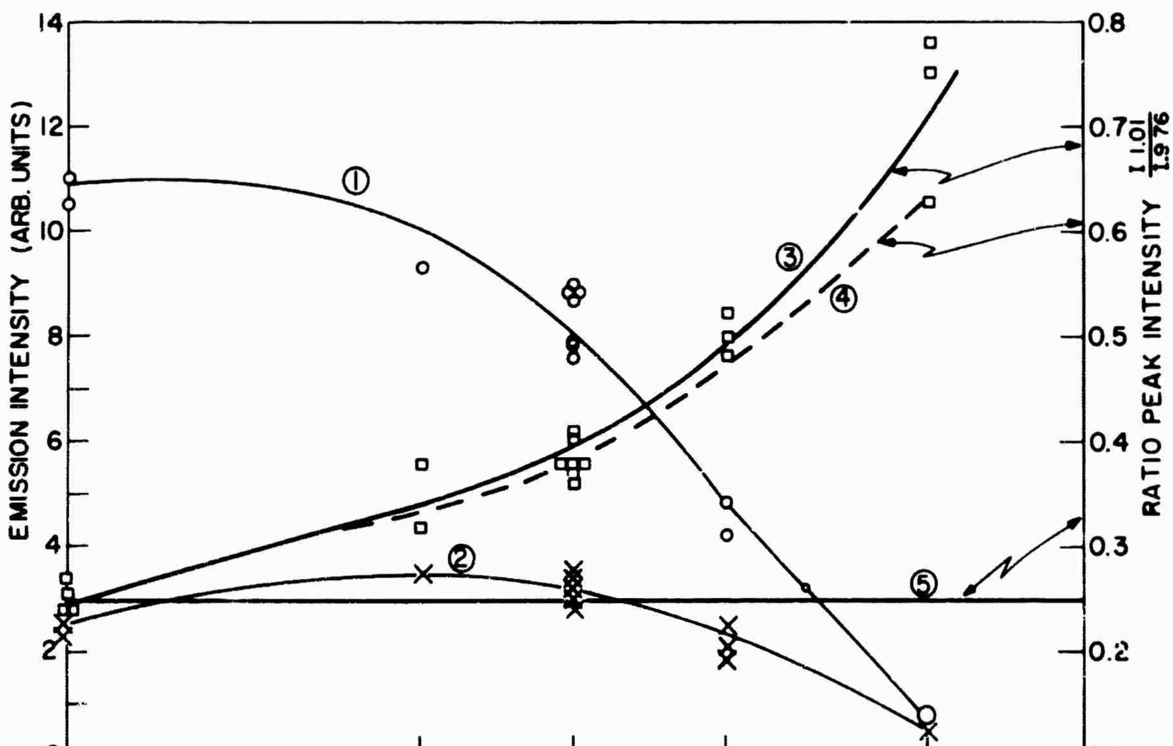

Figure 26 - Concentration Dependence of X-Ray Excited Luminescence of Yb^{+3}-Activated Li Mg Al SiO_3 Powdered Glass Samples at Room Temperature.

(1) Emission intensity of 0.976 μ band maximum; (2) Emission intensity 1.02μ band maximum; (3) Ratio of 1.02μ band maximum intensity to that of the 0.976μ band; (4) Curve (3) with the self-absorption correction made; (5) as discussed in text.

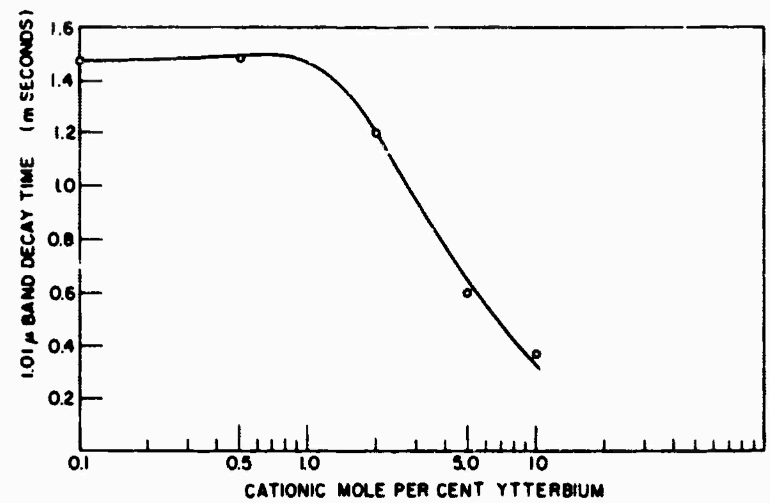

Figure 27 - Concentration Dependence of the Decay Time of the 1.02μ Emission Band in Yb^{+3}-Activated Li Mg Al SiO_3 Glass at 80°K.

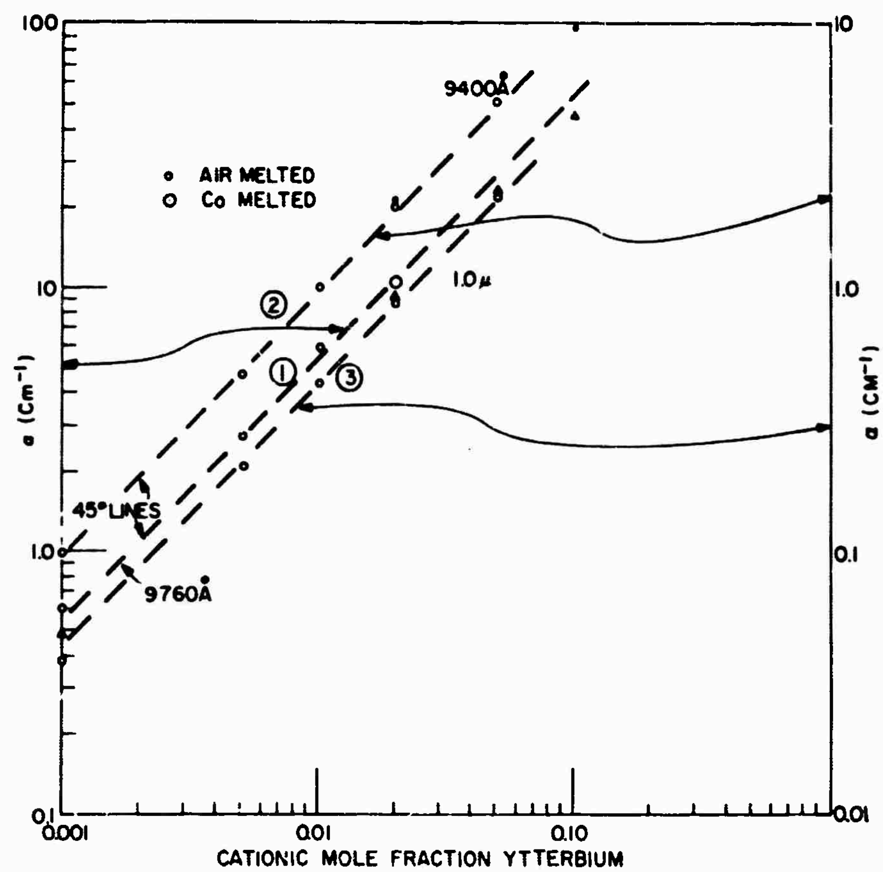

Figure 28 - Concentration Dependence of Absorption is Yb^{+3}-Activated Li Mg Al SiO_3 Glass.

(1) Absorption coefficient at 0.976μ; (2) Absorption Coefficient at 0.94μ; (3) Absorption Coefficient at 1.04μ.

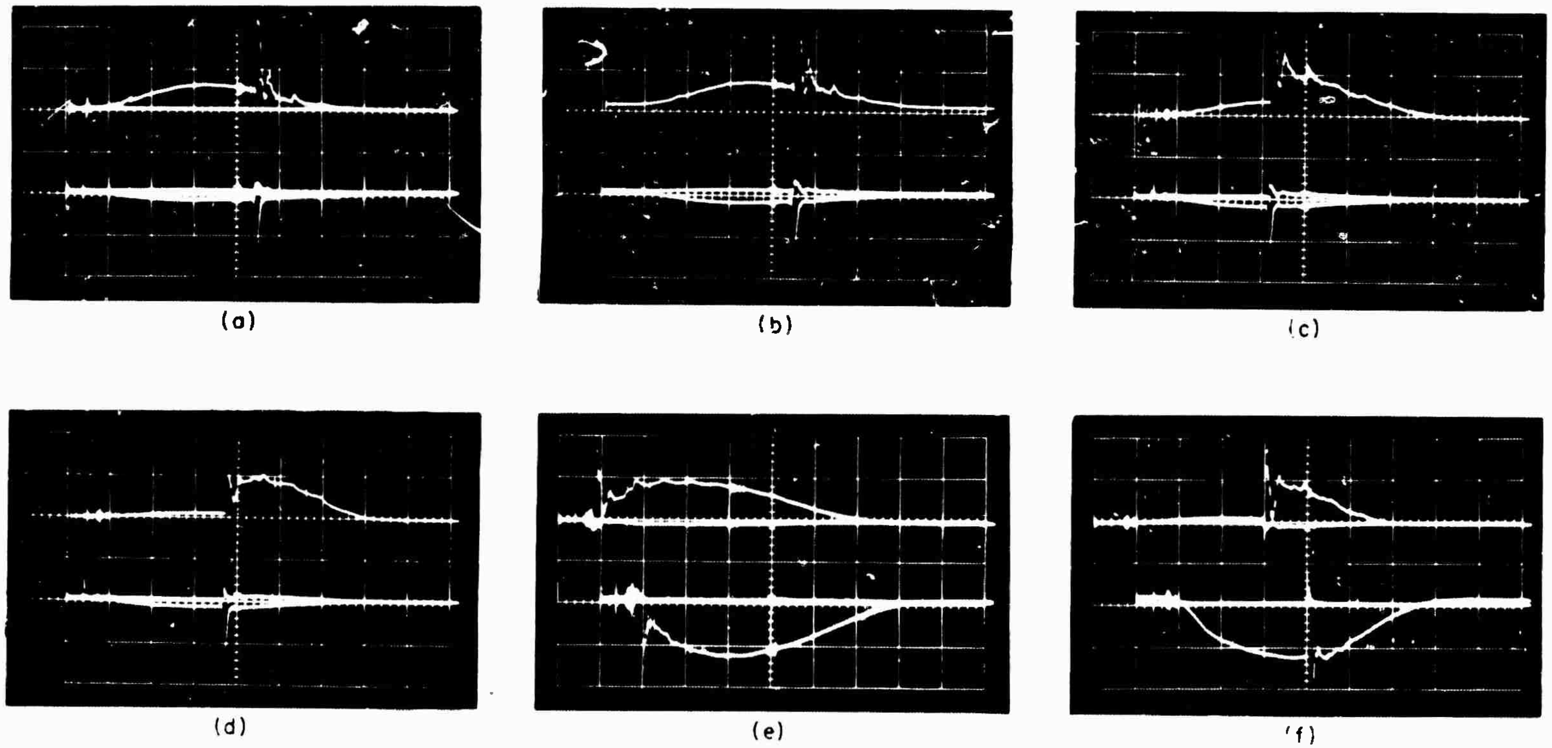

Figure 29 - Wavelength Dependence of Persistent Enhanced Ultraviolet Radiation from Double-pulsed Xenon Lamp

Conditions of excitation: Slow bank: 1.2kV, 280 f, 570 h, peak c .rrent density 2000 amp/cm^2. Fast Bank: 5kV, 14 f, no inductor, peak current density 25,000 amp/cm^2. Upper trace: 935 photodiode on output of monochromator (33A band pass) 200 sec per cm. writing speed. Lower trace: Lamp monitor as described in text.

(A) 4000A

(B) 3500A

(C) 3000A

(D) 2500A

(E) 2500A; fast pulse occurring first, showing that enhancement can persist over entire slow pulse period.

(F) 2500A; same as E but delayed fast pulse showing enhancement occurring during part of pulse only. (F) and (D) are identical, except for fivefold increase of gain in lamp monitor channel in (F).

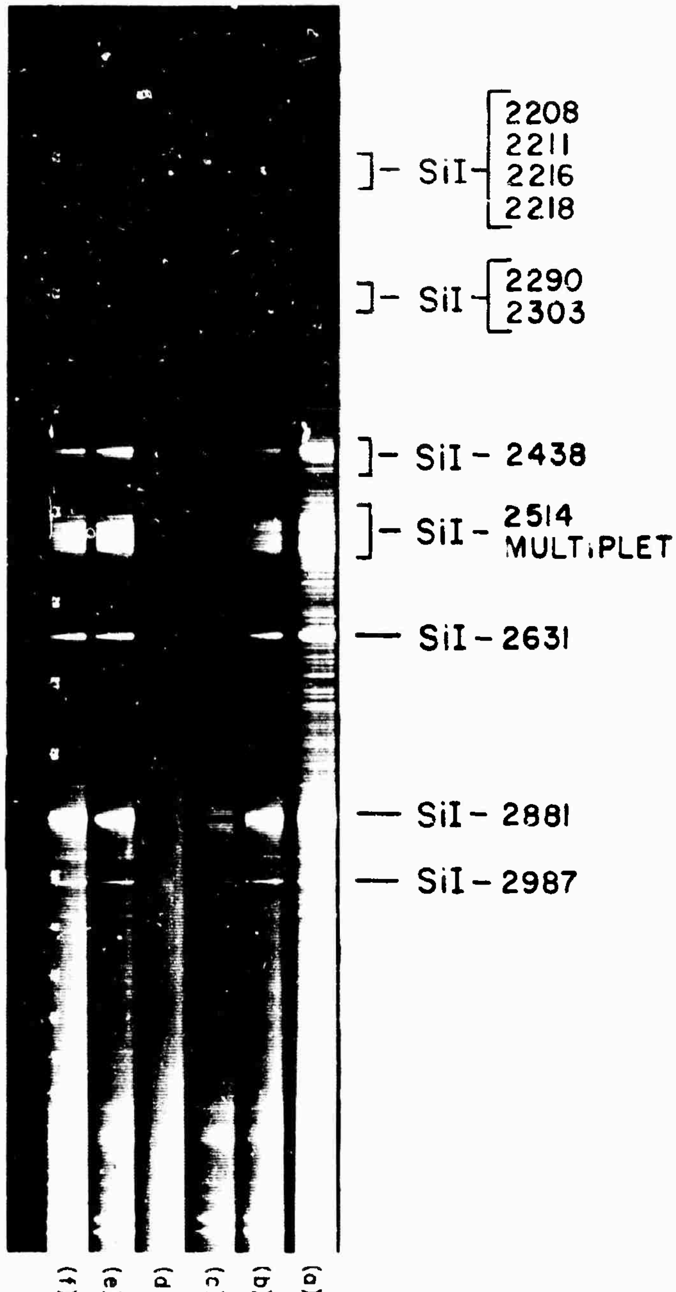

Figure 30 - Spectra of Gas-filled **Flashlamps.**
Conditions of Excitation:

Slow bank: 1.2 kV, 280 f, 570 h, peak current density 2000 amp/cm^2.

Fast bank: 5 kV, 14 f, no inductor, peak current density 25,000 amp/cm^2.

(a) Xenon flashlamp; slow pulse followed by fast pulse.
(b) Argon flashlamp; slow pulse followed by fast pulse.
(c) Argon flashlamp; fast pulse only.
(d) Argon flashlamp; slow pulse only.
(e) Argon flashlamp; fast pulse followed by slow pulses.
(f) Argon flashlamp; slow pulse followed by fast pulse.

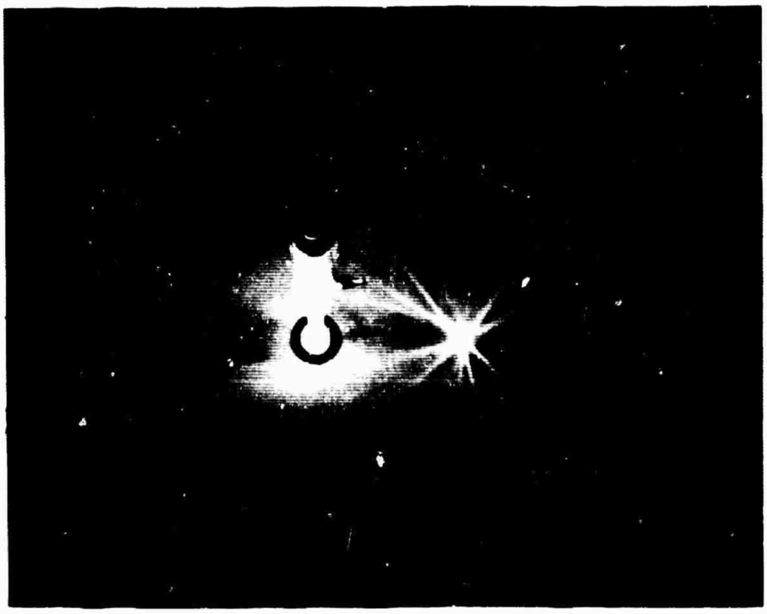

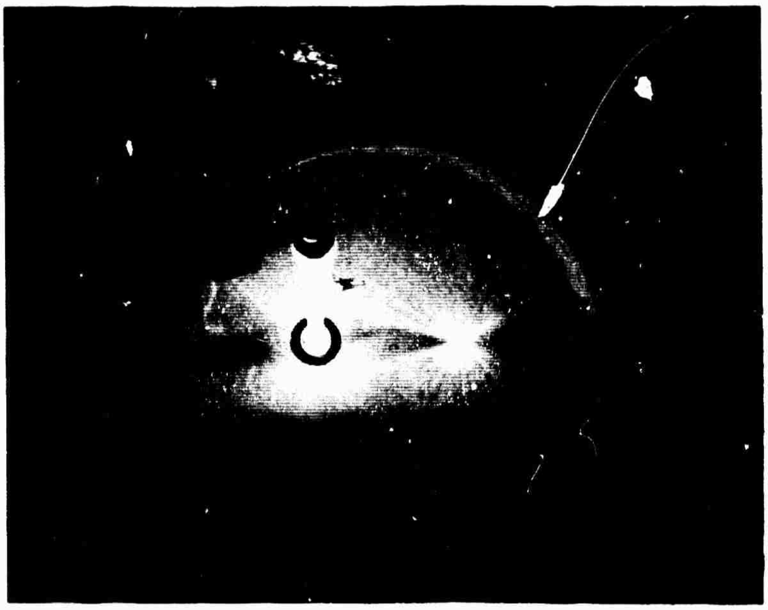

Figure 31 - Comparison of Molded and Machined Elliptical Reflectors. Upper picture: Relatively poor focus of the molded epoxy right elliptical cylinder, lined with aluminized mylar previously used in exploding wire pumping. Lower picture: Improved focus of the machined aluminum system, also lined with aluminized mylar. Dimensions of right elliptical cylinder: Focal distance $\cong$ 2-7/16" Major axis $\cong$ 7-3/16", Minor axis $\cong$ 6-3/4, Height = 2-7/8".

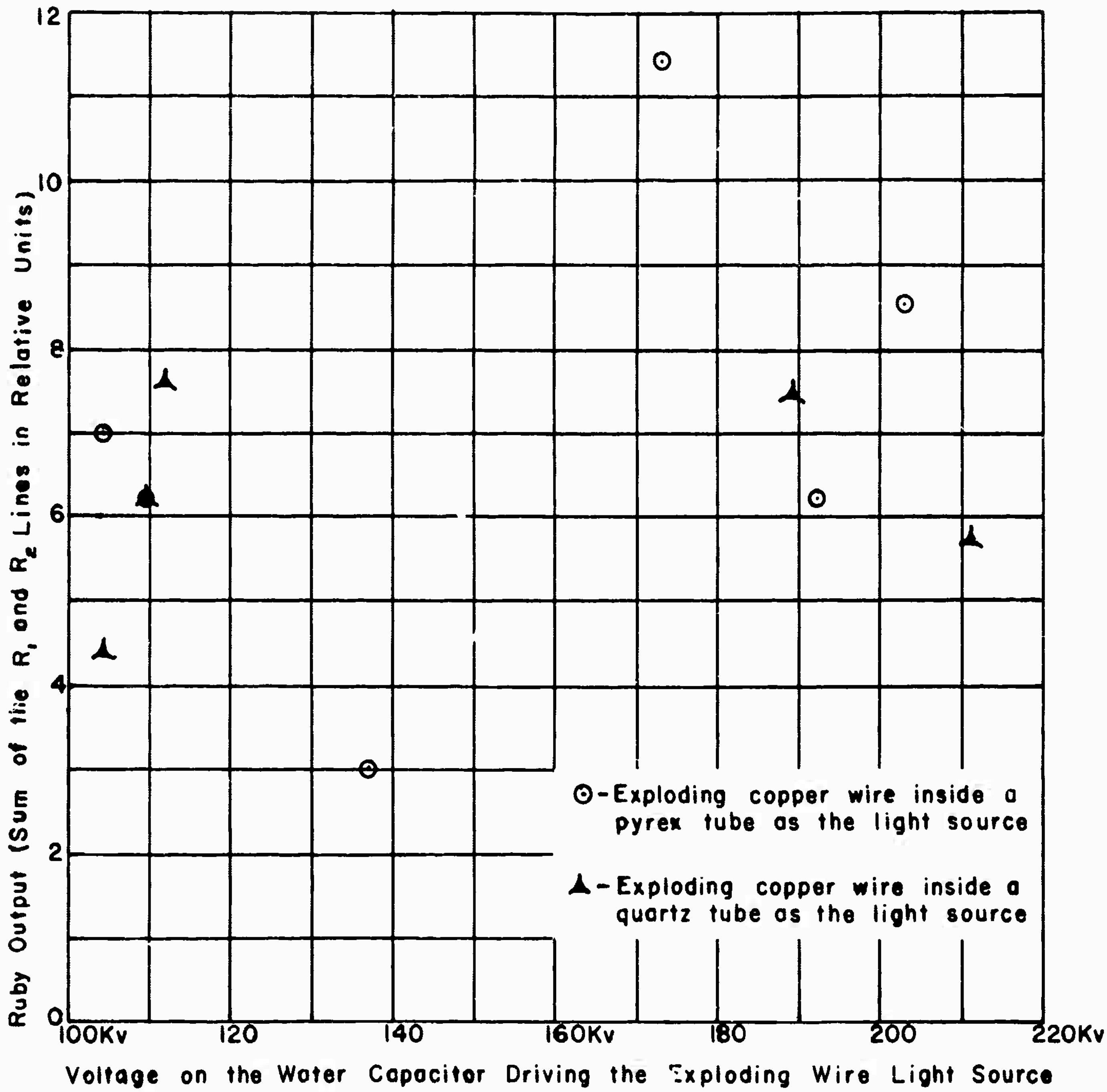

Figure 32 - Independence of Ruby Cutput of Optical Filtering of Exploding Ware Light Source. Note also the surprising result that the ruby output is essentially independent of voltage on the water capacitor. It is believed that this must be due to the wire plasma expanding more rapidly in the more energetic shots, with consequent poorer focus on the ruby. The total output of the wire plasma does increase with increase in applied voltage.